Cement and Concrete Research 41 (2011) 1208–1223

Contents lists available at ScienceDirect

Cement and Concrete Research

journal homepage: http://ees.elsevier.com/CEMCON/default.asp

Mechanisms of cement hydration

Jeffrey W. Bullard [a,*], Hamlin M. Jennings [b], Richard A. Livingston [c], Andre Nonat [d], George W. Scherer [e], Jeffrey S. Schweitzer [f], Karen L. Scrivener [g], Jeffrey J. Thomas [h]

[a] Materials and Construction Research Division, National Institute of Standards and Technology, Gaithersburg, MD, USA
[b] Department of Civil and Environmental Engineering, Massachusetts Institute of Technology, Cambridge, MA, USA
[c] Department of Materials Science and Engineering, University of Maryland, College Park, MD, USA
[d] Laboratoire Interdisciplinaire Carnot de Bourgogne (ICB), UMR 5209 CNRS-Université de Bourgogne, Dijon, France
[e] Department of Civil and Environmental Engineering/PRISM, Princeton University, Princeton, NJ, USA
[f] Department of Physics, University of Connecticut, Storrs, CT, USA
[g] Institute of Materials, Construction Materials Laboratory, École Polytechnique Fédérale de Lausanne, Lausanne, Switzerland
[h] Schlumberger-Doll Research, Cambridge, MA, USA

ARTICLE INFO

Article history:
Received 21 July 2010
Accepted 22 September 2010

Keywords:
Hydration (A)
Kinetics (A)
Microstructure (B)

ABSTRACT

The current state of knowledge of cement hydration mechanisms is reviewed, including the origin of the period of slow reaction in alite and cement, the nature of the acceleration period, the role of calcium sulfate in modifying the reaction rate of tricalcium aluminate, the interactions of silicates and aluminates, and the kinetics of the deceleration period. In addition, several remaining controversies or gaps in understanding are identified, such as the nature and influence on kinetics of an early surface hydrate, the mechanistic origin of the beginning of the acceleration period, the manner in which microscopic growth processes lead to the characteristic morphologies of hydration products at larger length scales, and the role played by diffusion in the deceleration period. The review concludes with some perspectives on research needs for the future.

Published by Elsevier Ltd.

Contents

* Corresponding author. National Institute of Standards and Technology, 100 Bureau Drive, Stop 8615, Gaithersburg, MD 20899, USA. Tel.: +1 301 975 5725; fax: +1 301 990 6891.
E-mail address: jeffrey.bullard@nist.gov (J.W. Bullard).

0008-8846/$ – see front matter. Published by Elsevier Ltd.
doi:10.1016/j.cemconres.2010.09.011

1. Introduction

Understanding the kinetic mechanisms of cement hydration intersects both academic and practical interests. From an academic standpoint, the chemical and microstructural phenomena that characterize cement hydration are quite complex and interdependent, making it difficult to resolve the individual mechanisms or the parameters that determine their rates. Fundamental study of hydration therefore offers significant scientific challenges in experimental techniques and multi-scale theoretical modeling methods. From a more practical standpoint, the drive to produce more sustainable concrete materials is leading to more complex mix designs that include increased amounts of secondary mineral additions, often originating as by-products of other industrial processes, and a wide variety of chemical admixtures that can enhance concrete performance. More complete knowledge of basic kinetic mechanisms of hydration is needed to provide a rational basis for mixture proportioning as well as the design and selection of chemical admixtures.

Several detailed reviews have been written about the mechanisms that are thought to govern the kinetics of hydration [1–4]. At the time they were published, several important issues – the mechanistic origin of the induction period, the rate-controlling mechanisms during the acceleration period, the most important factors responsible for the subsequent deceleration of hydration, etc. – were addressed but left unresolved due to either lack of data or seemingly equivocal evidence for different viewpoints. But significant strides have been made both in experimental techniques and in theoretical models in the intervening years. Our intention is to focus on these more recent developments, thereby providing an updated picture of the current state of knowledge and identifying the remaining controversies or gaps in understanding. Finally, we then propose a road map for future cement hydration research that targets the remaining gaps and could have the greatest impact toward supporting the development of more sustainable concrete materials.

2. Background

Models of chemical kinetics that are based on fundamental chemistry and physics at the molecular scale have been feasible for gas-phase systems [5], for nucleation of crystals from a melt or aqueous solution [6], and even for dissolution and growth at crystal surfaces [7–11] by analyzing and modeling the individual kinetic steps in detail. Similarly, a fundamental approach to understanding cement hydration would involve breaking the problem down to the study of the kinetics of the individual mechanistic steps. This approach is desirable because it would provide a foundation for understanding the interactions among the coupled processes, and for establishing how the microscopic kinetics lead to the development of the microstructure at higher length and time scales. Furthermore, mechanistic understanding at the molecular scale would provide knowledge of the dependence of rates of reaction and diffusion on temperature and the state of saturation, that is, the effect of curing conditions.

Cement hydration involves a collection of coupled chemical processes, each of which occurs at a rate that is determined both by the nature of the process and by the state of the system at that instant. These processes fall into one of the following categories:

1. *Dissolution/dissociation* involves detachment of molecular units from the surface of a solid in contact with water. A good comprehensive review of dissolution kinetics was performed by Dove et al. [12,13].
2. *Diffusion* describes the transport of solution components through the pore volume of cement paste [5,14] or along the surfaces of solids in the adsorption layer [15,16].
3. *Growth* involves surface attachment, the incorporation of molecular units into the structure of a crystalline or amorphous solid within its self-adsorption layer [17].
4. *Nucleation* initiates the precipitation of solids heterogeneously on solid surfaces or homogeneously in solution, when the bulk free energy driving force for forming the solid outweighs the energetic penalty of forming the new solid–liquid interface [6].
5. *Complexation*, reactions between simple ions to form ion complexes or adsorbed molecular complexes on solid surfaces [18,19].
6. *Adsorption*, the accumulation of ions or other molecular units at an interface, such as the surface of a solid particle in a liquid [15,16,19].

These processes may operate in series, in parallel, or in some more complex combination. For example, even simple crystal growth from solution involves diffusion of solute to the proximity of an existing solid surface, adsorption of the solute onto the surface, complexation of several solute species into a molecular unit that can be incorporated into the crystal structure and, finally, attachment and equilibration of that molecular unit into the structure [9,19]. When in series, these steps are coupled in the sense that the products of one step are the reactants of the next step, and so on. Often, but not always, one step has a significantly lower rate than any of the other steps in the sequence. In that case, all but the slowest step, *the rate-controlling step*, can reach equilibrium conditions and will determine the activities of the reactants and products of the rate-controlling step [19]. In this simple case where one step is rate-controlling, that step alone is responsible for the observed kinetic rate equation, the rate constant, and their temperature dependences. When the rates of two or more fundamental steps are comparable, then the rate equations and their dependence on system variables can be significantly more complicated and difficult to determine experimentally [19].

Unfortunately, the rigorous application of these concepts to cement hydration continues to be elusive because of the difficulty of isolating the individual chemical processes for detailed study. Even a task as seemingly simple as determining a fundamental rate law for the dissolution of Ca_3SiO_5, consistent with thermodynamics and the principle of mass action, is quite challenging because of the competing effects of rapid precipitation of less soluble phases from solution, the difficulty of adequately characterizing the surface at which dissolution is occurring and, even more basically, because rate data are usually acquired on polydispere particle suspensions without a complete characterization of the particle size distribution or absolute reactive surface area. The problem becomes exponentially more difficult to analyze when more complex systems like portland cement are contemplated. Therefore, for cement one has been forced to accept only partial knowledge about the net kinetic effects of multiple interacting processes.

The key to eventually building more mechanistic, less empirical models of hydration, capable of embracing its full range of chemical and structural complexity, is to develop strategies to isolate and study the individual rate processes that govern cement hydration. Such strategies will inevitably involve a close collaboration among a wide variety of experimental techniques, along with mathematical models and numerical simulation methods that can provide an intellectual framework for interpreting the data. This kind of collaboration has born fruit for unravelling the kinetics of certain processes in environmental geochemistry [10,20,21] and other branches of materials science [22–25].

2.1. Scope of this review

Nearly every review of portland cement (PC) hydration kinetics [1,2,4] spends the majority of its attention on the hydration characteristics tricalcium silicate, Ca_3SiO_5, or C_3S according to conventional

cement chemistry notation.[1] One reason is that the impure monoclinic polymorph of C_3S, referred to as alite, constitutes about 50% to 70% of PC by mass. Progress in basic understanding of kinetics is made more feasible by restricting attention to this simpler chemical subsystem because the analysis of chemical kinetics becomes increasingly complex with increasing number of components and phases. In addition, alite tends to dominate the early hydration period that comprises setting and early strength development because it is the component most responsible for formation of the calcium silicate hydrate gel (C–S–H), the principle product of hydration.

In keeping with this trend, much of the new progress in cement hydration research has been made either on pure C_3S or on alite itself. Recent research shows that triclinic C_3S has significantly different microstructure and hydration kinetics than impure, monoclinic alite [26]. Pure C_3S powders tend to be much finer grained than alite powders prepared and ground under similar conditions [26] because impurities in alite, mostly Mg and Al, promote grain growth during cooling from clinkering temperatures. In addition, some have speculated that the different crystal structure or impurity levels in alite alter the density of reactive sites at the surface, (e.g. screw dislocations or stacking faults) which can modify dissolution rates. Finally, there is some evidence that the growth morphology of C–S–H hydration products may be less porous, and therefore more resistant to mass transport, in C_3S pastes than in alite pastes [26]. This may be related to the experimental observation that hydration of C_3S often slows down markedly at lower degrees of hydration [27] than does hydration of alite [26].

Recent research on hydration of the C_3A + gypsum subsystem of PC will also be reviewed because of its importance in determining the calcium sulfate requirements of PC with and without replacement by mineral admixtures. This will include a discussion of the interactions among the silicate and aluminate subsystems that are important for understanding the influence of sulfate levels on the hydration kinetics of PC with partial replacement by fly ash or blast furnace slag.

In closing this section, it is helpful to mention the experimental techniques that have been used to monitor hydration kinetics, because these techniques will be referenced repeatedly in the remainder of the paper. Most of the techniques used to date monitor the *net rate* of hydration, that is the overall progress of hydration without regard to the action of individual chemical reactions. Such methods include isothermal calorimetry, continuous monitoring of chemical shrinkage, in situ quantitative X-ray diffraction, semi-continuous analysis of pore solution composition, nuclear magnetic resonance spectroscopy (NMR), quasi-elastic neutron scattering (QENS) and small angle neutron scattering (SANS). The relative merits and weaknesses of such methods have been thoroughly assessed elsewhere; being outside the scope of this review, the interested reader is referred to [28] for more details. For now, we note that none of these techniques resolves the details of any particular mechanism, but they have proven useful for comparing the hydration of different cements, for characterizing the influence of variables such as cement fineness, water-to-solids mass ratio (w/s), cement composition, temperature, and the type and dosage of admixtures. More importantly, comparison of different methods, such as calorimetry and SANS data [29,30], calorimetry and QENS data [31,32], or calorimetry and chemical shrinkage on parallel specimens can provide insights into the hydration process that cannot be obtained by any one method alone. For example, the SANS surface area tracks closely with the cumulative heat measured by calorimetry at very early times, up to about the peak hydration rate, but then diverges as the morphology of the C–S–H phase is not constant with time. The same is true of the constrained water component of the QENS signal.

[1] In this shorthand notation, single capital letters are used to denote oxide units, e.g. C = CaO, S = SiO_2, A = Al_2O_3, F = Fe_2O_3. We will use this convention frequently throughout the paper.

3. Mechanisms of C_3S or alite hydration

The rates of hydration of (triclinic) C_3S, alite, and even PC have long been observed to vary with time by orders of magnitude in a complicated, nonmonotonic fashion. Historically, this fact has led to the division of the overall progress of hydration into four or five stages, defined by somewhat arbitrary points on a plot of hydration rate versus time [4]. For our purposes in discussing kinetic mechanisms, we find it helpful to consider the four periods indicated in the calorimetry plot of hydration rate versus time shown in Fig. 1: (1) initial reaction, (2) period of slow reaction, (3) acceleration period, and (4) deceleration period. The beginning and ending of these stages are still difficult to pinpoint precisely, but they provide a more accurate picture of the current state of knowledge.

In this section we undertake a review of recent progress in experimental and theoretical research on cement hydration in terms of its mechanism(s) and implications for microstructure development. Attention is focused on results that have come to light in the last decade, with limited review of earlier work only where necessary for historical context. The interested reader may refer to [4] and references therein for a more comprehensive review of earlier work.

3.1. Initial reaction

The initial period is characterized by rapid reactions between C_3S and water that begin immediately upon wetting, characterized by a large exothermic signal in isothermal calorimetry experiments [26]. The heat released by wetting the cement powder contri butes to this early exothermic signal, but significant heat is also released by dissolution of C_3S. The enthalpy of congruent C_3S dissolution is −138 kJ/mol, based on the reaction [33,34]:

$$C_3S + 3H_2O \rightarrow 3Ca^{2+} + H_2SiO_4^{2-} + 4OH^- \quad (1)$$

Chemical analyses of the solution phases [35–39] have furnished persuasive evidence that C_3S dissolves congruently and quite rapidly in the first seconds after wetting. In dilute suspensions of C_3S, for example, the increase in silicate concentration over the first 30 s suggests that the dissolution rate may be at least 10 μmol m^{-2} s^{-1} [27]. Stein [40] calculated a theoretical solubility product for C_3S of $K_{sp} \approx 3$, when referenced to Eq. (1), which would imply that C_3S should continue to dissolve until reaching equilibrium calcium and silicate concentrations in solution of several hundred mmol/L. In fact, it is well known that C_3S dissolution rates decelerate very quickly while the solution is still undersaturated, by about 17 orders of magnitude with respect to the ion activity product of Reaction (1)

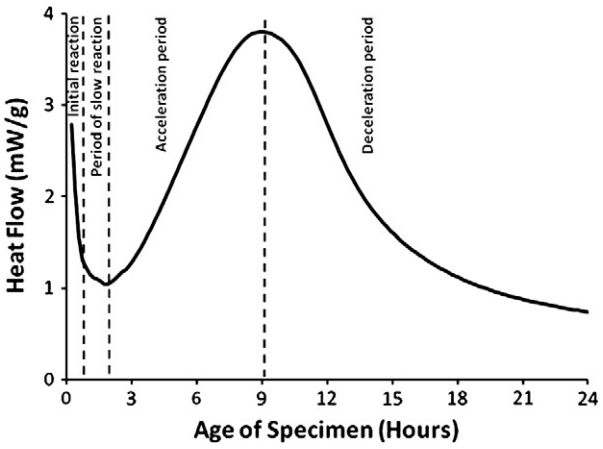

Fig. 1. Rate of alite hydration as a function of time given by isothermal calorimetry measurements.

compared to the equilibrium calculation, by the end of this period [27,40,41]. The mechanism of this early deceleration of C_3S has been a subject of considerable debate over the years, and many hypotheses have been proposed. The reader is referred to [4] and references therein for a description of the proposed mechanisms. Here we will focus on three mechanistic explanations that continue to have the greatest plausibility in light of recent experimental and theoretical research.

3.1.1. Metastable barrier hypothesis

Stein [42] and others [43] have argued that the deceleration is caused by the rapid formation of a continuous but thin metastable layer of a calcium silicate hydrate phase, which Gartner [2] has called C–S–H(m), that effectively passivates the surface by restricting its access to water, or restricts diffusion of detaching ions away from the surface. This thin layer is proposed to reach equilibrium with the solution at the end of the intial reaction period. Jennings [44] reviewed solution composition data from several decades of literature and showed that they tend to lie along one of two curves on a plot of calcium concentration versus silicate concentration, as shown in Fig. 2. The curve with higher Ca and Si concentrations was interpreted as reflecting equilibrium of the solution with a *metastable* hydrate layer having a variable Ca:Si molar ratio, and Gartner and Jennings [41] subsequently used the Gibbs–Duhem relation to estimate the Ca:Si molar ratio of this metastable hydrate as a function of calcium concentration in solution.

The metastable barrier hypothesis implies that the metastable hydrate isolates the underlying alite from the solution, which then comes into equilibrium with the hydrate. However, the mechanism for the end of the delay period is not evident. The fact that the time of the end of the slow reaction period has such a precise and repeatable value indicates that there must be some critical process acting during that period. This must take the form of some continuing chemical reaction or reactions that eventually destabilize the metastable layer in some way [2,4]. Indeed, calorimetry measurements show that the rate of heat output never decreases all the way to zero during the period of slow reaction.

Bullard [45] recently simulated the metastable barrier hypothesis for C_3S hydration, using a kinetic cellular automaton model of coupled reactions and diffusion phenomena using the principles of mass action and detailed balances. Simulations using the metastable barrier hypothesis adopted assumptions about the composition variability both of the passivating layer and of the more stable forms of C–S–H, based on limited and indirect experimental evidence. Even so, the simulations quantitatively reproduced a number of experimental observations of the evolution of the solution composition, the composition variablity of C–S–H, and the hydration rate of C_3S at two different water–cement mass ratios and initial conditions of the solution [27,46,47].

One difficulty with the metastable barrier hypothesis has been the scant direct experimental evidence of the existence of such a layer. However, the last several years have witnessed significant progress in this area. Nuclear resonance reaction analysis (NRRA), based on the ^1H ($^{15}N, \alpha, \gamma)^{12}$ resonance, has been used to measure the hydrogen depth profile at and below the surface of a specimen, with a depth resolution of a few nm and a sensitivity to hydrogen of a few μg/g [48,49]. By probing below surfaces of cementitious phases immersed in aqueous solution for different times, they have observed changes in the hydrogen depth profile as a function of time. Some typical depth profiles for hydrating triclinic C_3S are presented in Fig. 3. The profile is characterized by a Gaussian peak at the surface and a diffusion-like curve into the depth of the sample. The Gaussian peak has been interpreted as a thin but continuous hydrated layer [49]. Based on ideas from the glass corrosion literature, the overall hydrogen depth profile measured by NRRA has been interpreted as a set of layers with differing degrees of calcium/hydrogen exchange, as shown in Fig. 4. Although the Gaussian peak remains essentially fixed at later times (Fig. 3), the profile extends progressively deeper into the solid, reaching appreciable hydrogen concentrations as deep as 0.4 μm after 45 min at 30 °C. This increasing average penetration depth of hydrogen indicates that significant hydration reactions are still occurring during the slow reaction period. These conclusions are not too different from the mechanisms proposed in earlier publications [1,2,4,50].

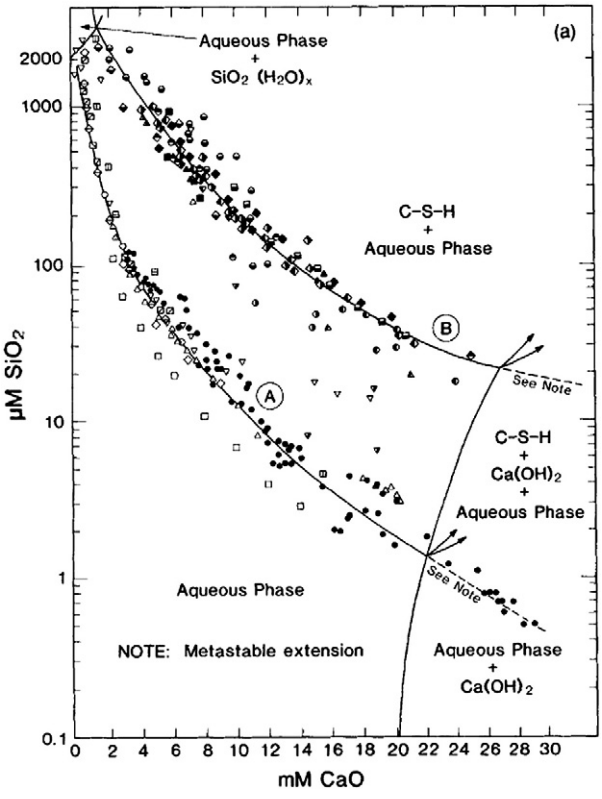

Fig. 2. Concentrations of silica (*y*-axis in μmol/L) and calcium (*x*-axis in mmol/L) reported for cement paste pore solution, collected from an extensive literature search in [44], and interpreted as indicating that either of two types of C–S–H can establish equilibrium with the solution.

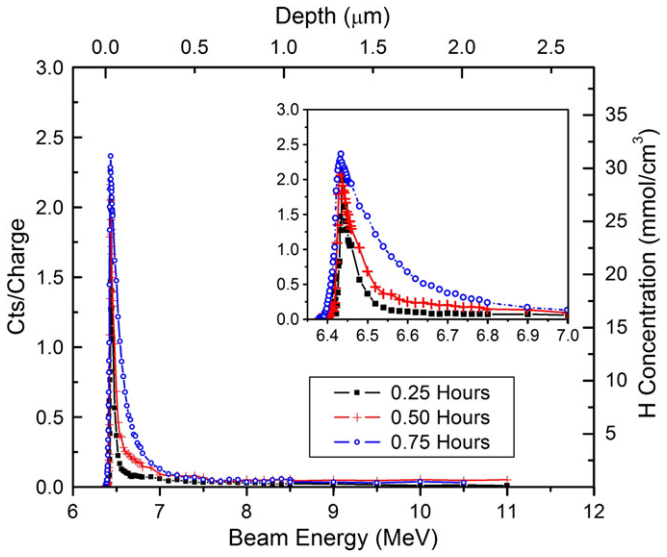

Fig. 3. Progression of hydrogen concentrations with depth and time during the initial and slow reaction periods for triclinic C_3S hydrated at 30 °C [49].

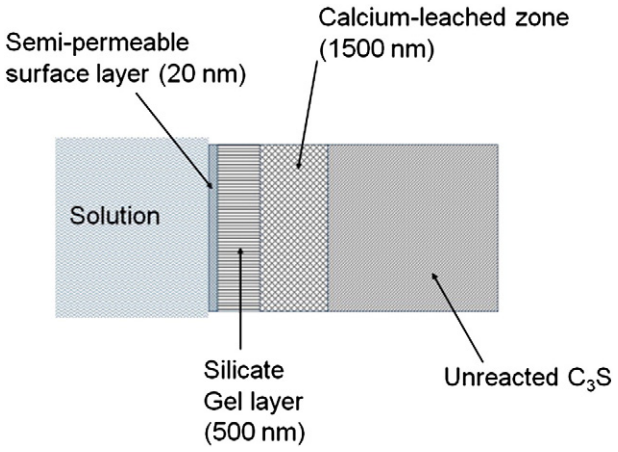

Fig. 4. Schematic diagram of the arrangement of surface layers on a C_3S grain during the slow reaction period based on the hydrogen depth profile measured by nuclear resonance reaction analysis (NRRA).

More recently, Bellmann et al. [51] have examined pastes and very dilute suspensions of C_3S nanoparticles in water. Using ^{29}Si NMR, they observed that an intermediate calcium silicate phase containing hydrated silicate monomers forms very early during hydration, a result that is consistent with earlier research on C_3S [50,52–54]. Their data demonstrate that, at least for nanoparticulate C_3S, hydration proceeds in two stages: formation of an intermediate silicate hydrate phase followed by conversion of this phase into C–S–H once the solution becomes sufficiently concentrated with calcium.

With greater direct evidence of the existence of an early hydrate phase, the challenge still remains to demonstrate that the phase has the necessary passivating influence on C_3S to explain the transition to the slow reaction period. NRRA data have been interpreted as indicating a thin surface hydrate that is permeable to calcium and water but not to silicates, although this latter idea is a conjecture because NRRA does not measure either calcium or silicate species. Moreover, the length of the slow reaction period has been correlated with the time required to achieve a critical hydrogen depth in NRRA experiments. For example, increasing temperature both shortens the slow reaction period and increases the rate of penetration of hydrogen below the surface (Fig. 3). And when sucrose, known to be a strong retarder, is added to the solution, the penetration rate of hydrogen below the surface occurs much more slowly than without sucrose [49]. All of these studies therefore provide strong evidence of a direct correlation between the length of the slow reaction period and the rate of development of the surface hydrate. A remaining challenge is to determine if the development of that surface hydrate controls the rate of hydration or if the rate of hydration controls the development of the surface hydrate.

If the metastable barrier hypothesis is correct, the layer must cover the great majority of the C_3S surfaces and be fairly dense if it is to effectively block the diffusion of one or more dissolved components. There are examples of nanoscale metal oxides such as alumina being able to passivate aluminum surfaces and limit further oxidation, but in those instances the layer is extremely stable thermodynamically and mechanically and has a close crystallographic relationship with the underlying metal, in contrast with the metastable C–S–H phase. Both atomic force microscopy conducted on flat C_3S surfaces under water [55] and high-resolution electron microscopy on dried samples [56] have been used to search for evidence of a continuous film of this kind. However, although patches of some kind of precipitate are often observed on the surfaces at very early times, evidence for a continuous layer has not been found using these direct methods of surface examination.

3.1.2. Slow dissolution step hypothesis

The metastable barrier hypothesis discussed in the last section assumes either explicitly or implicitly that the rate of C_3S dissolution in the period of intial reaction would continue to be rapid up to much higher solution concentrations of calcium and silicates if not for the formation of the passivating hydrate layer. However, other researchers have assumed that C_3S dissolution rates decrease rapidly for some other reason. Barret et al. [35,36] originally proposed that a "superficially hydroxylated layer" forms on C_3S surfaces in contact with water, and that the dissociation of ions from this layer occurs much more slowly than would be otherwise expected for a mineral in highly undersaturated solutions. Nonat et al. [27,39,47,55,57] have adopted this explanation for slow dissolution of C_3S and subsequently developed an alternative mechanistic explanation for the initial reactions that is based on a steady state balance between slow dissolution of C_3S and initially slow growth of C–S–H. According to these authors, the apparent solubility of the superficially hydroxylated C_3S is much lower than the one calculated for C_3S, and the dissolution rate decreases very rapidly when the calcium hydroxide concentration increases due to dissolution. When the solution exceeds a maximum supersaturation with respect to C–S–H, C–S–H nucleates very rapidly on C_3S surfaces and begins to grow slowly because of its initially low surface area. Growth of C–S–H causes the silicate concentration in solution to decrease and the Ca:Si molar ratio in solution to increase. Within minutes, a steady state condition is set up in which the solution is supersaturated with respect to C–S–H but undersaturated with respect to C_3S. Fig. 5 shows this behavior by superimposing the changes in solution concentration on a cross-section of a solubilty diagram in the system $CaO–SiO_2–H_2O$, with curves for both C_3S and C–S–H indicated in the figure. The dashed arrow in the figure indicates the trajectory of the solution concentration for pure congruent dissolution, which continues until a maximum supersaturation is reached with respect to C–S–H (point A in the figure). Nucleation of C–S–H causes the silicate concentration to decrease (bold arrow in the figure) as the solution composition approaches the solubility curve for C–S–H.

Evidence supporting this view comes from studies of dissolution rates of C_3S in stirred suspensions [58]. Increases in Ca and Si concentrations in solution were monitored continuously in suspensions of C_3S so dilute (w/s = 50,000) that, theoretically, the solution should never become supersaturated with respect to C–S–H. Without the complicating factor of C–S–H nucleation and growth, congruent dissolution caused the concentrations of Ca and Si to increase continuously in a 3:1 ratio. With this technique, initial C_3S dissolution

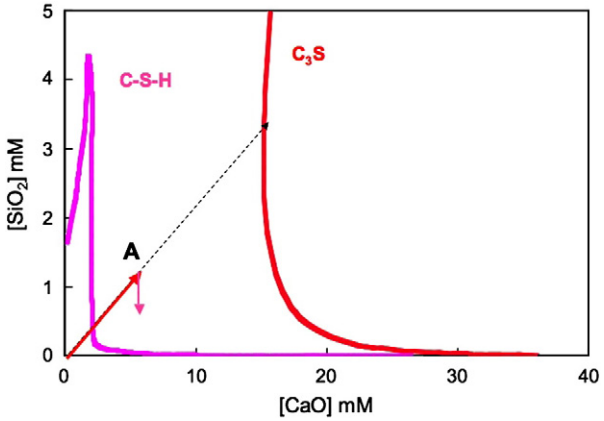

Fig. 5. Cross-section of a solubility diagram in the system $CaO–SiO_2–H_2O$. The arrow shows the path followed by the concentrations in solution during the congruent dissolution of C_3S. The concentration increases beyond the solubility of C–S–H until the maximum supersaturation from which C–S–H precipitates immediately is reached (point A). From [35,126].

rates were measured as approximately 10 μmol m^{-2} s^{-1} and the steady-state ion activity product (IAP) was estimated to be log IAP = −17 when referenced to Reaction (1), nearly 17 orders of magnitude less than the solubility product calculated from the Gibbs free energy of the reaction.

Along the same lines, the dissolution rates of many natural minerals in aqueous solutions do not follow a smooth relationship with respect to the saturation state of the solution [10,11,20]. Briefly, different mechanisms of dissolution are rate controlling depending on the saturation state of the solution. Far from equilibrium, high rates of dissolution are enabled by etch pit opening at surface defects, whereas closer to equilibrium but still significantly undersaturated, the driving force is insufficient to activate the etch pit opening and dissolution occurs primarily by a retreating step mechanism that is much slower.

This approach for low-solubility minerals has been applied to alite. Many experimental observations have shown that the rate of C_3S and alite dissolution is affected by the initial concentration of the solution [27,39,47,57]. Scanning electron microscope (SEM) observations of unground alite surfaces hydrated in different dilute solutions have further confirmed the importance of the initial saturation state. Samples hydrated in deionised water showed significant corrosion of the surface with the presence of small pits (hundreds of nanometers in diameter) whereas samples hydrated in saturated lime solution preserved a smooth planar surface [56]. Other studies performed on alite or cement pastes have also revealed the presence of pits at early times of hydration [59–61]. This mechanism of etch pit activation or deactivation, depending on driving force, implies that dissolution is a rate controlling mechanism and provides a satisfying way to make low dissolution rates of alite consistent with the considerable undersaturations at the end of the intial reaction period.

The slow dissolution step hypothesis for the onset of the period of slow reaction is supported by the observed roles of crystallographic defects in the early hydration processes of cementitious material, which have been studied by several researchers [62–64]. Maycock et al. [64] as well as Odler and Schüppstuhl [63] studied the effect of quenching rate on the reactions of alite and found that faster quenching, likely to induce more crystal defects, resulted in shorter induction periods. Fierens and Verhaegen [62] cooled C_3S at different rates from 1600 °C to 1300 °C before quenching, and similarly found that the duration of the induction period was related to the length of the thermal treatment. More recently, Juilland et al. [61]. performed a post-thermal annealing treatment at 650 °C on alite of narrow particle size distribution as a way to decrease the defect density. A change of polymorphism from monoclinic M3 to triclinic T1 occurred without any significant change of the particle size distribution. Isothermal calorimetry data for the annealed samples show the presence of a very long induction period for the thermally treated samples (Fig. 6), supporting the hypothesis that surface defects control the rate of dissolution and thereby influence the length of the induction period.

A difficulty with this slow dissolution step hypothesis is in reconciling the dissolution rates with the observed time dependence of silicate concentrations in the first minutes of hydration. Most experiments show a sharp peak in silicate concentration in the first minutes after wetting, which decreases almost as rapidly and is followed by a longer period of very slowly decreasing concentrations during the period of slow reaction. Before the peak, increases in silicate concentration can be interpreted as pure C_3S dissolution. The sharp decrease has been interpreted as the consumption of silicates due to nucleation of C–S–H [27]. Within 20 min, the silicate concentration decreases to about half its original value and continues to decrease much more slowly for the next 20 min. Therefore, one should expect the C_3S dissolution rates after 20 min to be comparable to the rates on the left side of the peak at the same silicate concentration in experiments where the calcium concentration is held fixed at 11 mmol/L, because at both those times the solution has basically the same composition and, therefore, the same driving force for dissolution [27,47]. However, such rapid C_3S dissolution rates are not experimentally observed after the initially sharp decrease in silicate concentration until the acceleration period begins. One possible explanation is that the C_3S surfaces on the right side of the silicate peak are already significantly covered with C–S–H precipitates, so that the dissolution rate per unit area may be rapid but the overall dissolution rate low.

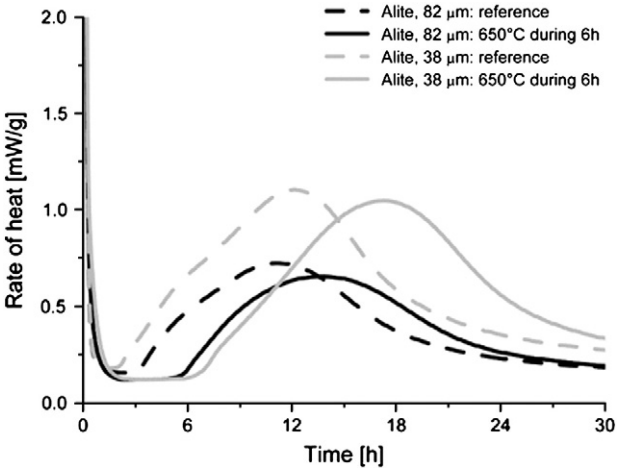

Fig. 6. Heat evolution of alite untreated (reference, dashed line) and treated at 650 °C for 6 h (plain lines) of narrow particle size distribution. All measurements were performed at 20 °C and the w/s ratio was kept at 0.4.

3.2. Acceleration period

In unretarded, unannealed C_3S and alite systems, the delay period is just the minimum in the hydration rate that is reached after the initial reaction but before the beginning of accelerated growth of hydration products [4]. A true induction period appears to exist as a distinct stage only when chemical retarders are added or materials have been annealed. Furthermore, this delay seems to be just the consequence of the slow reaction (due to one of the mechanisms described previously) until a critical point is reached when the rate of nucleation and growth starts to accelerate. Therefore, we have made the unconventional choice of omitting a separate section for the period of slow reaction, preferring instead to consider its aspects only in terms of the consequences for the onset of the acceleration period, which is generally agreed to be related to a nucleation and growth (N + G) mechanism.

Throughout this N + G period of hydration of C_3S and alite, the hydration rate, expressed as the time derivative of the degree of hydration,[2] $d\alpha/dt$, increases as α^r, where $2/3<r<1$ [4]. By analogy to autocatalytic chemical reactions, this behavior implies that the rate of hydration in this stage depends on the amount of some hydration product, presumably C–S–H. Supporting this idea, a large and growing body of experimental and modeling evidence [4,27,30,35,37,55,65–68] indicates that the rate-controlling step of hydration during this period is related to the heterogeneous nucleation and growth of C–S–H on alite and perhaps on other mineral surfaces as well. The evidence for this comes from a number of sources. C–S–H is observed to be formed primarily on surfaces of C_3S or alite [4,69,70] when observed by scanning, atomic force, or transmission electron microscopy. In addition, Zajac [71] has reported experimental measurements showing that the hydration rate of C_3S is proportional to the surface area of C–S–H as measured by nuclear magnetic

[2] We define the degree of hydration as the mass of C_3S consumed divided by its initial mass.

resonance (NMR) spectroscopy. If growth of C–S–H is rate-controlling, the hydration rate is expected to be proportional to the number of active growth sites for C–S–H (i.e., its surface area). Another paper in this issue [72] describes the application of various modeling and simulation methods that strongly support the underlying mechanism as being one of nucleation and growth and discusses in detail various hypotheses regarding the nucleation process (initial or ongoing); growth (isotropic, anisotropic or diffuse) and other mechanisms.

3.2.1. Timing of C–S–H nucleation

As already discussed, earlier reviews of cement hydration have concluded that the nucleation of a stable form of C–S–H occurs some time after the formation of a metastable hydrate layer on alite surfaces, and that the growth of the stable C–S–H precipitates happens by conversion of the metastable layer, whether directly or by a through-solution mechanism. Experimental and modeling studies over the past 10 years, described in Section 3.1, have cast some doubt on the necessity of this conclusion and indicate that nucleation and growth of C–S–H can occur at very early times and may not require a pre-existing hydrate phase.

Direct observations of the first C–S–H nucleation events in C_3S or alite systems are difficult to make. Conclusions drawn in the recent literature are mostly based on inferences from model interpretations of experimental data. For example, Garrault and Nonat [27] use the slow dissolution hypothesis and interpret the decrease in silicate concentrations in the opening seconds or minutes of hydration as the result of C–S–H nucleation, setting up the subsequent balance between C_3S dissolution and C–S–H growth. Application of the Avrami model to isothermal calorimetry or QENS data requires assuming an induction period of at least 1 h prior to any C–S–H nucleation to obtain good fits [73,74]. But both Thomas' application of a boundary nucleation and growth (BNG) model to fit isothermal calorimetry data [65] and its application by Scherer et al. to fit chemical shrinkage data [75,76] indicate that initial C–S–H nucleation occurs close to the time of mixing. The interested reader is referred to the companion paper [72] for more detail on the use of the BNG model for fitting these kinds of experimental data.

Bullard [45,48] used a kinetic cellular automaton model to simulate the microstructural development and solution chemistry during C_3S hydration using either the metastable layer hypothesis or the slow dissolution step hypothesis for the initial reaction and delay period, and found that only heterogeneous nucleation of C–S–H on C_3S surfaces could account for experimental observations of the evolution of the solution composition and degree of hydration. Those simulations also differentiated between heterogeneous nucleation and growth of C–S–H, and indicated that nucleation occurs in a fairly short burst over only a few minutes, either at the end of the initial reaction when assuming the slow dissolution step hypothesis or near the onset of the N + G period when assuming the metastable layer hypothesis. The narrow window of C–S–H nucleation occurs in the simulations because nucleation consumes calcium and especially silicates from solution, thus lowering the saturation index of C–S–H enough that the thermodynamic driving force for growth of existing precipitates is less than the energetic barrier to nucleation.

The importance of (stable) C–S–H nucleation as a controlling factor in early-age hydration of C_3S is underscored by experiments reported by Thomas et al. [67] in which C_3S pastes were seeded by adding a reactive form of C–S–H at the time of mixing. In those experiments, the induction period was essentially eliminated and hydration progressed to N + G kinetics immediately and at a higher rate than in an unseeded paste. Earlier, Wu and Young [77] attributed the accelerated rates of hydration of C_3S by colloidal silica to C–S–H nucleating on the surface of the silica particles. These results show that the timing of the onset of accelerated rates characterized by the N + G period depends primarily on having enough growing regions of C–S–H to give an appreciable hydration rate. Without seeding, more time is needed for the natural nucleation and growth process to provide enough C–S–H surface area for appreciable growth rates to be observed. Since the definition of an induction period is a time prior to initial nucleation, the slow early hydration period of unretarded paste should not be so labeled if slow growth of stable C–S–H is indeed occurring during that time.

NMR data earlier from Clayden et al. [52] and more recently from Bellmann et al. [51] suggest that dimeric species of silicate only start to be detected at the end of the slow reaction period. This suggests that the polymerization of silicate may be an important mechanism in the transition to nucleation and growth kinetics.

3.2.2. C–S–H growth mechanism and morphology

It seems well established that growth of C–S–H controls hydration kinetics from the delay period until some time after the rate maximum. The growth mechanism must be closely related to the observed development of C–S–H structure either as the aggregation of nanoscale particles [78–82], or as large but defective sheets of silicate layers [83]. Gartner [83] proposed a mechanism of growth for branching sheets, which would be consistent with observed kinetics of hydration. This mechanism involves the attachment of silicate tetrahedra at growing silicate chains all along the perimeter of 2D silicate sheets and the incorporation of calcium and hydroxyls in the layers between these sheets to form a tobermorite-like or jennite-like structure. Each existing embryo after nucleation grows in this fashion, and as growth continues the layers form regions of well-ordered, crystalline structure on a length scale of about 5 nm. However, as the sheets grow in 2D, the probability of building a defect into the layer increases with the number of growth sites. The lattice strain caused by a growth defect can cause the sheets to buckle and diverge away from each other, thus causing a disordering of the crystalline structure. This mechanism is generally compatible with the observed kinetics, and the concept that nanograins of C–S–H may actually be domains of bonded but defective calcium silicate layers could explain the high cohesive strength of C–S–H and the observation that the nanograins do not coarsen appreciably despite having exceedingly high surface area.

An alternative theory of C–S–H growth is based on the aggregation of C–S–H nanoparticles to form an interpenetrating fractal structure. In this scenario, C–S–H solid particles grow only to a certain characteristic size, on the order of a few nanometers, at which point they stop growing and remain stable for extended periods of time. However, existing C–S–H nanoparticles either can stimulate the heterogenous nucleation of new particles on their surfaces or the aggregation of previously nucleated C–S–H nanoparticles from the solution [67]. A difficulty with this idea is that both heterogeneous nucleation on existing surfaces and homogeneous nucleation of nanoparticles in solution requires a higher driving force (i.e. supersaturation of the solution) than continued growth on the existing C–S–H surfaces. However, chemical models and experimental observations indicate that the supersaturation is high enough to cause C–S–H nucleation from solution only in the first minutes of hydration [27,54,68]. Unless C–S–H formation is controlled by nucleation of a stable C–S–H by in-place transformation of a metastable C–S–H [2], nucleation is likely confined to very early times.

For mature pastes, the Jennings colloid model [79,81,82] envisions two stable morphologies of C–S–H with different packing densities, known as high density (HD) and low density (LD) C–S–H, which is supported by experimental observations such as nanoindentation [84,85]. Moreover, the packing density might be signficantly lower during the early hydration period and then increase with time. Since the observed hydration kinetics during the N + G period depend in part on the rate at which the available space is filled, this becomes an important kinetic variable, which was considered in the mechanisms proposed by Bishnoi and Scrivener [86] to explain the effect of particle size on the early kinetics, and by Thomas et al. [30] to explain

the greater amount of early hydration of C_3S observed with $CaCl_2$ acceleration.

3.2.3. What triggers the onset of N + G?

Gartner et al. [4] list four proposed mechanisms for the beginning of noticeably accelerating hydration rate after the delay period, shown in Table 1. Each hypothesis has received substantial support in the literature, and experimental data have been produced that argue for or against each one. The topic is still controversial, and we will try only to bring the debate up to the present day with the most recent experiments and models.

It should be noted that N + G models assume that both the rate of growth of individual regions of product in any linear direction are constant with time, as are the rate of nucleation of new product regions (per unit of untransformed volume or boundary area) Thus these models imply that the variation in the overall hydration rate with time occurs only due to changes in the total amount of interface between product regions and the solution. This assumption also requires that the driving force for nucleation and for growth be relatively constant with time, at least during the period around the main hydration peak when the nucleation and growth models fit the data closely. It further implies that the rate of C_3S dissolution is controlled by the rate of nucleation and growth, and not the other way around. Both the metastable barrier hypothesis and the slow dissolution step hypothesis can explain this dependence of dissolution rates on C–S–H nucleation and growth. The metastable barrier hypothesis proposes that the metastable layer around the C_3S particles has a higher solubility than stable C–S–H and controls the solution concentrations of calcium and silicate ions. As stable hydration product precipitates from the pore solution, the metastable layer continuously dissolves at its outer surface to replenish ions to the solution, while simultaneously reforming at its inner surface by C_3S dissolution, a process that continues at least until all of the particle surfaces are covered with hydration product (i.e. after the main rate peak). According to the slow dissolution step hypothesis, the delay period is caused by low dissolution rates when the solution composition is not sufficiently undersaturated with respect to C_3S. During the acceleration period, both C–S–H and CH are present and their increasing rates of growth continuously remove ions from solution which must be replenished by further dissolution of C_3S.

As already described, a preponderance of experimental evidence indicates that some form of C–S–H exists prior to the end of the slow reaction period, likely being formed near the beginning of that period. Therefore, it is difficult to see how nucleation of C–S–H, by itself, could be the trigger for the acceleration period. In this connection, it is worthwhile recalling that ^{29}Si NMR detects silicate dimers only at the end of the slow reaction period [51]. Although the technique is not very sensitive to small quantities, the dimerization of silicates indicates a possible change in the structure of C–S–H at the end of the slow reaction period. Therefore, the view that continuous nucleation and growth of C–S–H alone causes the transition from slow reaction to acceleration should be revisited to see if a change in the structure of existing C–S–H embryos could further enhance accelerated growth beyond that caused by the increase in surface area of the product.

Table 1
Possible causes of the onset of the N + G period, reproduced from [4].

Hypothesis/mechanism	Brief description
Nucleation and growth of C–S–H	Nucleation and growth of a stable C–S–H happen at the end of the slow reaction period and are rate-controlling during the acceleration period as a metastable protective layer of hydrate becomes chemically unstable and exposes the high-solubility C_3S.
Growth of stable C–S–H	Nuclei of stable C–S–H, already formed during initial reaction, grow at a nearly exponential rate. C–S–H growth is rate controlling. No metastable hydrate barrier layer is invoked.
Rupture of initial barrier	Metastable C–S–H barrier layer is semipermeable. Solution inside is close to saturation with respect to C_3S. Osmotic pressure leads to its rupture
Nucleation of portlandite (CH)	Nucleation and growth of portlandite become rate-controlling (and thus indirectly control the rate of growth of C–S–H)

Of the four mechanisms listed in Table 1, mechanical rupture of a surface barrier has been argued to be most consistent with the NRRA results described in Section 3.1.1 [48]. If the barrier layer is permeable to Ca^{2+} and water but impermeable to silicate ions, the accumulation of a silicate-rich gel, less dense than C_3S, could exert a swelling pressure against the surface barrier. By this hypothesis, a critical volume of gel is eventually reached at which the barrier ruptures, allowing the trapped silicate ions to react with the calcium-rich solution. This enables the rapid development of outer product C–S–H throughout the N + G period. If a protective surface layer is indeed ruptured due to pressure exerted by an underlying silica gel, the critical volume of the gel needed for rupture has not yet been determined. However, the critical volume should depend only on the physico-chemical properties of the surface layer and the substrate, and therefore in particular should be independent of the w/s ratio of the paste.

A fourth proposed mechanism for the end of the induction period, the delayed nucleation and precipitation of CH, was suggested by Young et al. [87]. This hypothesis does not invoke a surface barrier layer, but instead is based on the observation that during the induction period the solution is supersaturated with respect to CH, and after the induction period the Ca^{2+} concentration drops rapidly. The maximum supersaturation of the solution with respect to CH (i.e. ratio of the ion activity product to the solubility product of CH) at the onset of the N + G period is often observed to be about 4.5 to 5 for pastes with w/s ~ 1 when proper care is taken to calculate the activities corresponding to the measured concentrations of Ca^{2+} and OH^- and to account for the presence of the $CaOH^+$ complex.

Since 1989, the CH nucleation hypothesis has become less popular in light of experimental data that were thought to contradict it. For example, seeding a C_3S paste with small particles of CH produced no accelerating effect [88] and may even retard C_3S hydration [89]. Similarly, hydration of C_3S in lime water is retarded at early ages relative to hydration in initially pure water [90]. Furthermore, when dilute suspensions of C_3S are hydrated in an aqueous solution in which the calcium concentration is maintained just below the saturation point of CH [27,47], the hydration kinetics followed the typical trends shown in Fig. 1 despite the fact that portlandite could not nucleate in the suspensions. The same is true of the NRRA experiments discussed earlier [48,49] in which the specimens were in contact with a lime water solution from the beginning.

More recent experimental research [56] and modeling studies [68] have shown how the CH nucleation hypothesis can be reconciled to these seemingly contradictory experimental results. If slow C_3S hydration during the delay period is due to the slow dissolution step hypothesis, instead of the metastable barrier hypothesis, then the higher concentration of calcium and hydroxyl ions, caused by the presence of CH seeds or by the use of lime water, will lower the driving force for dissolution of C_3S. This will slow the dissolution rate of C_3S and consequently increase the delay time. However, if very high supersaturations with respect to portlandite could be produced initially, then portlandite nucleation and C–S–H nucleation and growth can occur without the need to dissolve as much C_3S. The greater quantity of C–S–H could lead to acceleration at these higher lime concentrations even though retardation is observed at lower lime concentrations. In fact, this phenomenon has been observed experimentally [91].

In closing this section, we note that almost ten years ago, Gartner et al. [4] stated that the four hypotheses listed in Table 1 have "coexisted somewhat uneasily" in the literature, awaiting more definitive experimental tests. In the intervening years the experimental investigations and advances in modeling we have described have allowed much more quantitative and detailed analysis of the phenomena occurring in the periods of slow reaction and acceleration. Unfortunately, even this more advanced scrutiny has not settled the issue decisively. Aspects of more than one have been demonstrated to be plausibly consistent with observed changes in rate and chemical composition of the pore solution. This is an area where progress will depend on continued advances in the characterization of the structural and kinetic properties, both in terms of new experimental methods and more sophisticated multi-scale computer modeling techniques.

3.3. Deceleration period

Even though the period of "post-peak" decelerating hydration progress (Fig. 1) is important in concrete technology because of the slower strength development, there have been comparatively few quantitative studies of this later period. It is widely considered that at later ages the rate of hydration is controlled by a diffusion process. However, several other factors may also be important, namely:

1. consumption of small particles, leaving only large particles to react;
2. lack of space, or
3. lack of water.

The third factor is particularly important in practice. The total volume of hydrates is slightly less than the combined volume of the reacting cement plus water (by about 5% to 10%). This decrease in total volume, known as chemical or le Chatelier shrinkage, leads to the formation of gas-filled porosity after setting and a decrease in internal relative humidity, which will decrease the hydration rate. Therefore, the analysis of kinetic data in this period must consider whether the system was in contact with a water reservoir or was sealed from external sources of water.

The effect of particle size distribution is not only important during the main hydration peak, but after it as well. In a typical cement, the size of the initial particles ranges from around 50 μm to 60 μm down to smaller than 1 μm. Particles less than about 3 μm are completely consumed by about 10 h and particles below 7 μm by 24 h [92]. Knudsen argued in 1980 [93] that the simultaneous hydration of different particle sizes obscures the rate controlling mechanism. His argument is probably applicable only at later times, because the mechanisms of nucleation and unobstructed growth of C–S–H depend only on the total surface area and are therefore not obscured by a range of particle sizes. Nevertheless, to eliminate complications due to broad particle size distributions, Costoya [26] and Bishnoi and Scrivener [86] adopted the practice of studying alite divided into different particle size fractions.

The time dependence of the cumulative amount of reaction sometimes has a distinct "knee", as shown by a plot of the bound water index (BWI) inferred from QENS measurements in Fig. 7. This knee, when observed, is often assumed to correspond to the onset of diffusion. Supporting this idea, mathematical fits of BWI versus time often indicate a transition to a parabolic time dependence at the knee. On the other hand, the transition is not always as obvious as in Fig. 7. Even in QENS studies, the knee is not as exaggerated as in Fig. 7 when three populations of bound water are considered [74,82,94] when calculating BWI instead of only two [31]. The transition is even less evident from cumulative data. In fact, neutron scattering data track calorimetry data closely until shortly after the main peak, but the two curves sometimes diverge afterward [29,31,74]. One reason may be that calorimetry primarily measures the exothermic dissolution of C_3S, while neutron scattering tracks microstructural features of

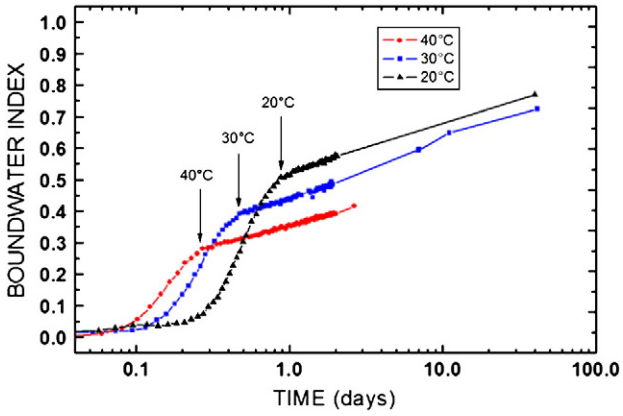

Fig. 7. Plots of bound water index (BWI) versus time for C_3S hydration measured by quasi-elastic neutron scattering [31].

the hydration products (e.g. states of water) as a proxy for reaction progress. This difference in the way changes are measured may mean that the knee observed in QENS data may reflect the onset of some change in the hydrated microstructure rather than a transition in the rate of reaction. But it is important to note that the knee *does not* coincide with the maximum observed rate of hydration, $d\alpha/dt$. The $d\alpha/dt$ maximum is in fact the inflexion point in the cumulative curve, where there is no indication of a change in rate controlling mechanism.

From this and other evidence, it now seems very unlikely that a transition to diffusion rate control is responsible for the first period of deceleration immediately after the main peak, although diffusion may becom rate controlling at later ages. The inevitable impingement of different domains of the growing hydration product, which is a fundamental feature of nucleation and growth transformations, reduces the surface available for growth and readily explains the shift from accelerating to decelerating hydration rate (see full discussion in [72]). Based on hydration simulations conducted according to boundary nucleation and growth conditions [65], Bishnoi and Scrivener [85] recently proposed that the shape of the main hydration peak results from the fast outward growth of a diffuse, highly porous C–S–H product.

The transition to diffusion controlled kinetics, if it occurs at all, likely happens well after this period of initial impingement and when heat release rates decrease to nearly zero. Such a transition in rate control would occur due to the formation of thick product layers that hinder the transport of reactants. Because this is a microstructural effect, it is useful to look at the overall development of micro- and nanostructure for clues. Allen et al. [30,95,96] have shown using SANS that there are surface fractal and volume fractal length scale regimes associated with the deposition of nanoscale C–S–H onto the hydrating particles, and Mori et al. [97] have inferred a gradual change in fractal dimension of C–S–H gel from a surface fractal at early ages to a volume fractal at the transition point, which they associate with thickening of the layer of hydration products around the hydrating C_3S. In addition, examination of microstructures by scanning electron or scanning-transmission electron microscopy often indicate either gaps or regions of low-density product adjacent to the reacting grain surfaces [98–100], while hydration products evidently deposit further away from the grains. These kinds of microstructural features imply that there may not always be a significant barrier to the transport of chemical species to and from the reacting grains. Other indirect evidence against the hypothesis of pure diffusion control can be found in the work of Peterson and Juenger [74], who used QENS to examine the hydration of C_3S in water and in solutions of $CaCl_2$ or sucrose. They analyzed the cumulative progress of reaction characterized by the bound water index (BWI) and fit the curves with an empirical model,

in the spirit of the Avrami model, that divided hydration kinetics into three stages: (1) an induction period at early times, (2) a nucleation and growth period at intermediate times, and (3) a diffusion-controlled period at later times. In this case, the later time period extended only to about 48 h after mixing, which is still relatively early in the hydration process. Their fits indicated that the diffusion coefficient for C–S–H must vary by more than an order of magnitude depending only on whether triclinic or monoclinic C_3S is used as the starting powder. A similar point was made by Bishnoi and Scrivener [86]. They found that, to model the kinetic data for alite powder with different particle sizes, it was necessary to assume that the diffusion constant varied considerably with particle size. Since C–S–H grows by a through-solution process, it is difficult to explain how the source of the solute species or the particle size distribution could influence the properties of C–S–H so strongly. This suggests instead that the pure diffusion model used to fit the data is incorrect.

Other QENS data seem to indicate that filling of the capillary pore space cannot entirely account for the later age kinetics of C_3S hydration. The available pore space in cement paste is essentially defined by the initial amount of water in the mix [50]. The reaction progress variable $\beta(t)$ described by Livingston et al. [101] is the ratio of water consumed to the initial water in the mix, so this variable should reach unity when the pores are finally all filled, assuming that the cement mix has the ideal molar H/C_3S ratio of 3.1 which provides just enough capillary pore volume to accommodate the hydration products at complete hydration. However, the experimental evidence contradicts this; for example, the value of $\beta(t_D)$ for the curves presented in Fig. 7 never exceeds about 0.51. Thus the asymptotic kinetic behavior apparently cannot be explained by complete filling of the capillary pore space with hydration product. Livingston et al. used QENS to further investigate the effect on the asymptotic behavior of varying the w/s ratio. They found that the transition time, t_D, was independent of the w/s ratio and, in fact, that the individual curves could be collapsed into a single master curve by a simple vertical scaling that has a linear correlation with the w/s ratio. They concluded that the pore-filling mechanism could not be solely responsible for the transition to parabolic kinetics at later times. These same authors went on to propose an alternative mechanism for the transition point based on the hypothesis of rapid surface layer development that is complete at the end of the initial reaction period. If this interpretation were correct, the degree of reaction progress achieved at later times would be largely determined by the extent of the reaction during the delay period.

4. C_3A, aluminate phase and portland cements

In portland cements, which are the basis of well over 99% of cement used, the phase other than alite that most affects the hydration kinetics in the first few days is C_3A. The reaction of C_3A in the absence of calcium sulfate is very fast. Unlike alite, there is no period of slow reaction and setting is almost instantaneous. The first hydrates formed have been reported to be poorly crystallized aluminum hydroxide or AFm[3] phases, generally described as C_2AH_8 and C_4AH_{13} [50,102–104], although solid solutions or intercalated mixtures of these phases probably occur. With time, these metastable phases transform to the stable product — hydrogarnet, C_3AH_6. This transformation begins within 25 min near room temperature [102] and the rate of transformation increases with temperature. This quick setting behavior is undesirable in concrete, where a period of workability is needed before setting to allow the concrete to be placed. For this reason a source of calcium sulfate is added to cements to control the reaction of the aluminate phase, and this latter system will be the main focus in this section. The calcium sulfate added is generally in the form of gypsum ($CaSO_4\cdot 2H_2O$), but anhydrite ($CaSO_4$) is often also present in most natural sources of gypsum. The hemihydrate form ($CaSO_4\cdot 0.5H_2O$, mineral name bassanite) may also be present due to partial dehydration of gypsum during grinding.

In the presence of a source of calcium sulfate the pattern of reaction of C_3A is dramatically changed, as shown in Fig. 8 [105]. There is an initial period of rapid reaction, after which the rate decreases rapidly within a few minutes. During the intital reaction, ettringite ($C_3A\cdot 3CaSO_4\cdot 32H_2O$) is the main hydrate phase formed. This initial period of rapid reaction quickly gives way to a period of low heat output, the length of which depends on the quantity of calcium sulfate in the system. When the added calcium sulfate has all been consumed, the rate of reaction rapidly increases again, with calcium monosulfoaluminate as the main product phase. In cements, the period of slow reaction of C_3A should persist until well after the main rate peak of alite to ensure correct setting and hardening.

The main question regarding the hydration mechanisms of C_3A in the presence of calcium sulfate is the reason for the rapid slow down of the intitial reaction. There are three possible explanations:

1. The product phase ettringite slows the reaction by forming a diffusion barrier at the C_3A surfaces
2. Some other phases, for example AFm, slows the reaction in the same way
3. The reaction is slowed down directly by adsorption of some solute species provided by dissolution of calcium sulfate.

Most textbooks, following the early literature [3,50,106], attribute the decelerating rate to the formation and thickening of a barrier of ettringite crystals. However, as pointed out by Scrivener and Pratt [107], the morphology of ettringite as hexagonal rods is unlikely to provide a substantial barrier to ion transport. Direct observation of the early reaction of C_3A with sulfate in a transmission electron microscope wet cell shows a few scattered rods in the solution (Fig. 9). When samples are dried for examination in the SEM, the rods collapse onto the surface, but even in this configuration, the packing of rods is highly porous.

Scrivener and Pratt [107] earlier observed a disorganized layer directly on the surface of the reacting C_3A grain; they conjectured that this “gel like” layer could be responsible for slowing down the reaction. However the study of Minard et al. [105] clearly showed that this product is an AFm type phase, which also forms when C_3A is hydrated in the absence of calcium sulfate, where there is no retardation of C_3A dissolution. Furthermore, they found that there was more formation of this AFm phase when C_3A was hydrated with gypsum, compared to hydration with hemihydrate, where hardly any

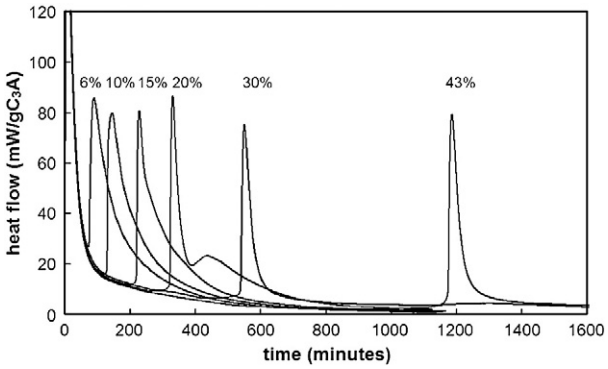

Fig. 8. Heat evolution rate curves during the hydration of C_3A (L1) in solutions saturated with respect to portlandite (liquid-to-solid mass ratio = 25) carried out with increasing quantities of gypsum, from [105].

[3] AFm phases (Al_2O_3–Fe_2O_3-mono) have the general formula $[Ca_2(Al,Fe)(OH)_6]\oplus X^-xH_2O$, where X represents a formula unit of a singly charged anion or a half unit of a doubly charged anion [100].

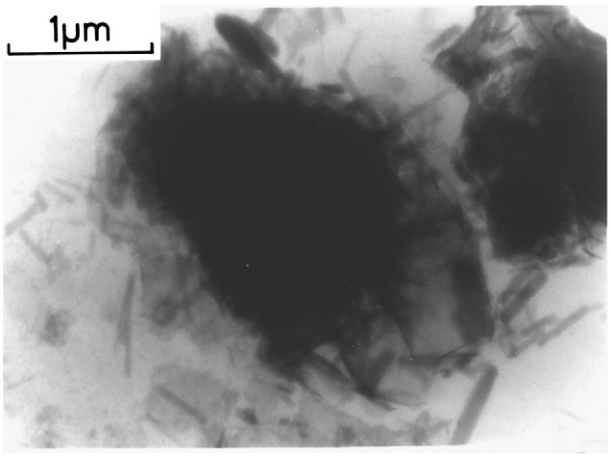

Fig. 9. Grain of C_3A in the presence of calium sulfate after 10 min hydration in environmental cell at high accelerating voltage [92].

AFm phase was formed. In contrast, the deceleration in reaction was more rapid with hemihydrate than with gypsum.

By process of elimination – the first two possibilities having been discredited – Minard et al. [105] attributed the early deceleration of C_3A reaction to the adsorption of sulfate ions on the surface of C_3A. This can also explain why the reaction slows down more quickly with rapidly soluble hemihydrate than with more slowly dissolving gypsum. For the reaction of C_3S, the slowing down of the reaction due to the build up of ions in solution has been discussed already in Section 3, and the important role of defects has been indicated there as well. A similar process could occur in the reaction of C_3A with calcium sulfate, whereby sulfate ions adsorb at defect sites and inhibit the formation of etch pits, so slowing down the rate of dissolution.

The length of the slow reaction period for the C_3A + sulfate system has been reported to increase approximately as the square of the initial sulfate/aluminate ratio of the system [3,106]. In contrast, Minard et al. [105] showed that the length of the period of slow reaction varies roughly linearly with the amount of calcium sulfate, although the situation is complicated by the dispersion of particle sizes. A linear relationship implies that ettringite formation and sulfate consumption during this period occur at a roughly constant rate that is controlled by dissolution of C_3A. A linear dependence would further support the conclusion that the reduction in rate is due to a change in dissolution rate and not to a barrier layer in which case the rate would be expected to decrease as the amount of hydration products increase.

When all the added calcium sulfate is consumed, the depletion of sulfate ions in solution causes a net desorption of the sulfate ions from the C_3A surface in an attempt to re-establish dynamic equilibrium between the adsorbed species and the solution. Therefore, a rapid increase in the dissolution rate is observed. This explanation also is more logical than the hypothesis that a barrier layer of ettringite is responsible for slow C_3A reaction because experiments show that the reaction rate increases *before* the ettringite starts to be consumed by the ongoing reaction. Furthermore, the amount of ettringite declines quite gradually in favor of the more stable monosulfate phase after sulfates are consumed from solution, whereas the large increase in reaction rate of C_3A happens over a much narrower time interval.

The period of renewed dissolution of C_3A, following the consumption of sulfates, leads to the formation of calcium alumino monosulfate according to the reaction:

$$2C_3A + C_3A\cdot 3CaSO_4\cdot 32H_2O + 4H_2O \rightarrow 3(C_3A\cdot CaSO_4\cdot 12H_2O)$$

The shape of the calorimetry peak for this reaction is quite different from that of the main hydration peak for alite, the former having an almost vertical acceleration part followed by an exponentially decaying shoulder. Interestingly, the shape of this peak is similar to that observed in the hydration of calcium aluminate (CA) cements, which is another system where crystalline hydration products form.

4.1. Interaction between silicates and aluminates

In a properly sulfated portland cement, the second aluminate peak in a calorimetry scan should occur after the main alite hydration peak (at around 10 h). This was discussed by Lerch as early as 1946 [108] (Fig. 10). It is important to note that he studied a cement with a high C_3A content (around 14% by Bogue). With a low SO_3 addition of 1.3% by mass, a large and sharp peak, corresponding to the reaction of the aluminate phase to form calcium monosulfoaluminate, occurs early and the reaction of alite is both delayed and suppressed. With 2.4% SO_3 addition, which he claimed corresponds to proper sulfation, the typical alite reaction peak occurred first and was followed shortly thereafter by a large and sharp peak corresponding to the $C_3A \rightarrow$ monsulfoaluminate reaction. However, for a cement with 3.5% SO_3, which is a C_3A to sulfate ratio more typical of modern cements, calcium monosulfoaluminate was not detected until 50 h. (We note, however, that Blaine finenesses of modern cements are also often significantly higher than in Lerch's time, and finer cements tend to have higher "optimum" SO_3 requirements.) The large and sharp calorimetry peak associated with monosulfoaluminate formation in the cement with 2.4% SO_3 addition is often confused with a shoulder peak seen after the main silicate peak (Fig. 11). Although this shoulder peak corresponds to the point of exhaustion of solid gypsum, at which point aluminate phase hydration accelerates significantly, the main aluminate hydration product at this time still appears to be ettringite, perhaps formed from sulfate previously absorbed in the C–S–H phase [100]. In Fig. 11 a subsequent low broad peak can be seen between about 20 h and 30 h, which appears to correlate with the formation of AFm phase(s). The mineral chemistry can become quite complex at this stage because any of several AFm phases can form, depending on temperature and the availability of carbonate ions or other anions such as chlorides. Even with only sulfate present, one assumes that monosulfoaluminate forms first but this can ultimately convert to a solid solution with hydroxyaluminate.

These observations indicate the apparent complexity of the interactions between the alite and aluminate phases during hydration. Such complexity highlights the need for simulation tools that can deal with the interactions among phases through the ions in the pore solution and the occupation of space by the hydrated phases.

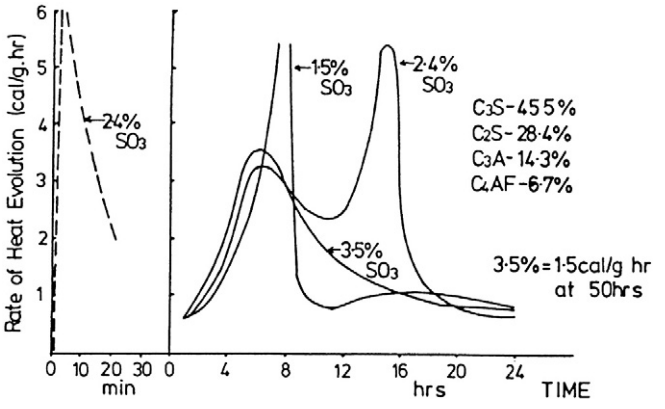

Fig. 10. Calorimetry of portland cement with different addition of gypsum. Reprinted, with permission, from theASTM Proceedings (1946), copyright ASTM International, 100 Barr Harbor Drive, West Conshohocken, PA 19428 [108].

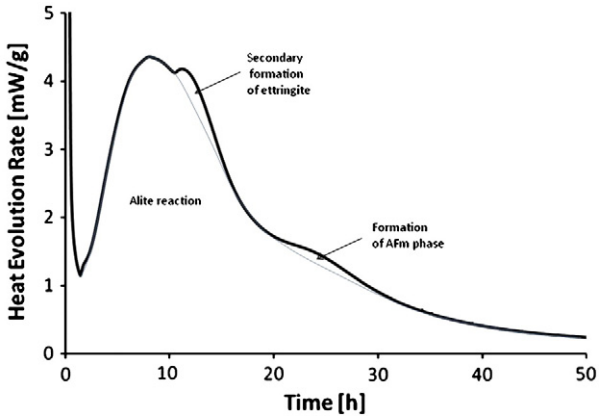

Fig. 11. Calorimetry curve of modern portland cement, showing typical shoulder peak where a secondary formation of ettringite occurs and subsequent broad peak corresponding to the formation of AFm phase.

5. Perspectives for future research

5.1. Motivation

As discussed in this review, cement hydration kinetics has been the subject of extensive investigation and yet the controlling mechanisms remain controversial. It is worth reviewing a couple of reasons for the importance of studying and understanding kinetics, apart from simple intellectual curiosity, as this helps motivate specific questions and research directions. Because the study of kinetics is a tool for elucidating mechanisms, it complements microstructure analysis by indicating which processes are predominant when structural changes occur. There are at least two broad areas of practical impact: 1) defining ways of controlling the rate of reaction, and therefore the rates of hardening and heat generation, and 2) finding ways of controlling and monitoring the structure and distribution of products; in short, controlling the microstructure and therefore *all* the material properties as a function of time. The first impact is related to controlling the length of time concrete remains fluid before it begins to gain strength and then the rate of subsequent strength development. The second has a more subtle, and potentially equally important, impact in the quest to control properties by manipulation of the micro- and nanostructure of concrete.

As for the rate of reaction, it is often stated that an ideal concrete should stay fluid during transport and placing and then very rapidly gain strength and other engineering properties. Both the mineralogy of cement and the addition of admixtures are used to control the kinetics of setting and hardening, but there is little consensus on the mechanisms, and chemicals are tested largely by trial and error. A mechanistic understanding would provide a powerful tool in the quest for new chemicals that are inexpensive, effective, noncorrosive toward steel reinforcing bars, and able to control equally the length of time before hardening starts and the rate of property development afterward.

Control of the microstructure of concrete has advanced remarkably in recent years, with the development of ultra-high strength products, such as Ductal®,[4] where the particle size distribution has been optimized on the basis of theoretical models. In contrast, the ability to control the microstructure of C–S–H has received relatively little direct attention, with a few exceptions [67,109]. Thus the morphology and spatial distribution of the products formed during the hardening of cement paste cannot yet be controlled with the same precision as for metals and other materials, but a mechanistic understanding should provide new strategies for predicting the evolution of microstructure and properties, and ultimately designing microstructure and properties.

While the control of microstructure has not been investigated very much, a few studies have correlated morphology with time of formation, i.e. the stage during which the product seems to form. During the 1980s, several papers [110–115] reported that specific morphological features seem to form during each stage of reaction. The C–S–H needle morphology that typically forms preferentially during the early stages was once seen as a clue to the reaction mechanism [110,113], but this has not stood the test of time. Gartner [83] and others [69,100] have analyzed morphology and established plausible relationships between kinetics and atomic structure.

An important aspect of recent progress on hydration kinetics is that the proposed mechanisms have been described in increasingly quantitative terms, which enables better comparisons to data. However, some very important questions remain almost completely unanswered. For example, with a few isolated exceptions [30], knowledge of the mechanisms that control the rate of reaction have not been applied to explain the sometimes dramatically altered rate of reaction, as well as altered microstructure and properties, which often accompany the use of admixtures. This includes accelerators and retarders, mineral admixtures of all kinds and variation in cement composition.

This review has identified several rate phenomena that can control hydration kinetics at different times:

1. Dissolution of cement
2. Diffusion of reactants to site of chemical reaction
3. Nucleation of first product
4. Growth of product, perhaps by “autocatalytic” formation of grains of product and which may be limited by chemical reaction or by diffusion of reactants to reaction site

The fact that more than one step can control the rate of reaction, depending on the stage of the reaction and perhaps on the presence of admixtures, in itself makes the mapping of the overall hydration process more complex than it would be if the rate were controlled by one step with a single activation energy. This suggests that the reaction kinetics might be best analyzed using a flow chart type of approach, an example of which is shown in Fig. 12, where the rate controlling step can be identified from among several candidates by evaluating several “if–then” type of statements. For example, the presence of seed clearly removes the nucleation step as being rate controlling, and also stimulates growth of product in the volume of water filled as opposed to just on the surface (at least this is one interpretation of the kinetic data). Neither dissolution of cement nor diffusion of reactants appears to be rate controlling throughout most of hydration, but rather the rate of product growth appears to control the rate at least until the product becomes congested in the capillary pore space at later ages.

As the modern drive for more sustainable concrete pushes the formulation of cement toward increased use of supplementary cementitious materials (SCMs) like fly ash and slag, concrete producers are faced with an ever more complex chemical and structural design space within which to formulate binders. Responding to the demand to replace greater volumes of portland cement with SCMs, producers are increasingly faced with “incompatibility” in the mixes, that is, unexpected and unexplained acceleration or retardation in the kinetics, combined with undesirable strength gain, shrinkage, and cracking. The impact of SCMs on hydration and kinetics is considered in more detail in another paper in this issue [116]. However, it is worth noting that scientific understanding of the

[4] Certain commercial equipment and/or materials are identified in this report in order to adequately specify the experimental procedure. In no case does such identification imply recommendation or endorsement by the National Institute of Standards and Technology, nor does it imply that the equipment and/or materials used are necessarily the best available for the purpose.

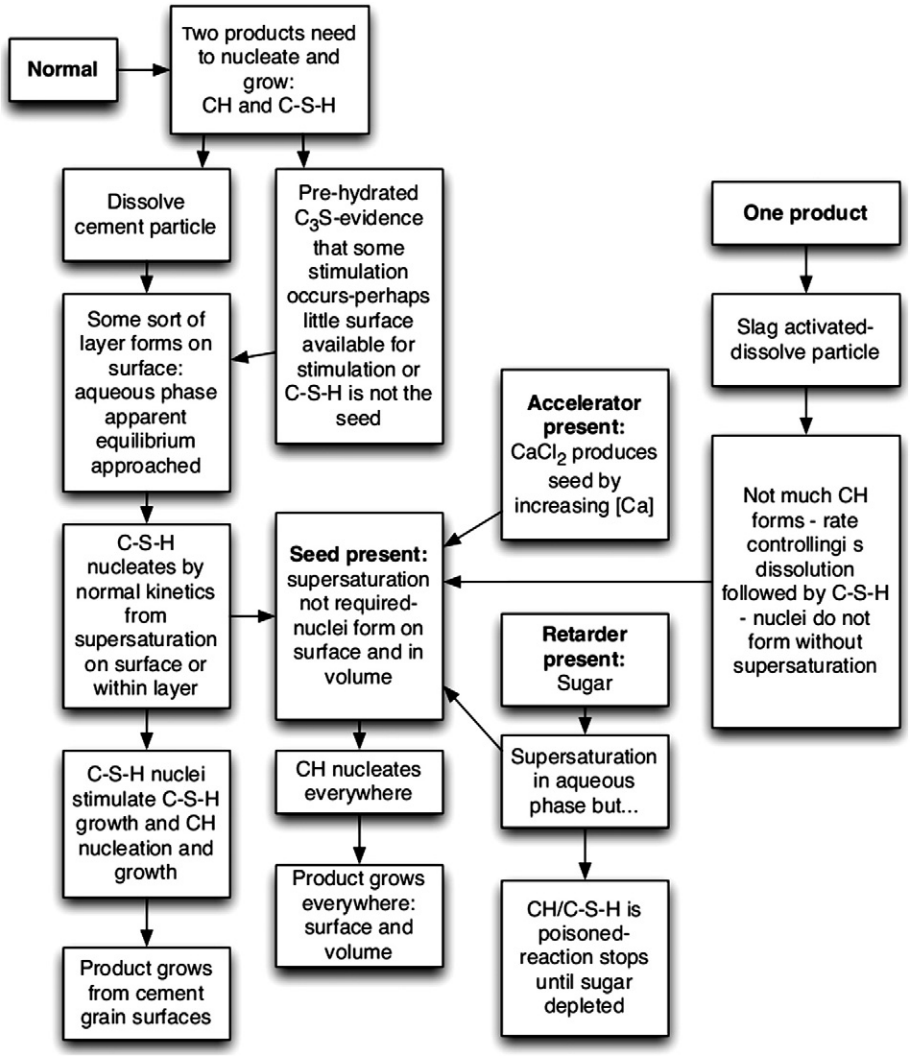

Fig. 12. Flowchart for organizing thinking about hydration kinetics and mechanisms.

influence of SCMs on cement hydration is still in its infancy, even though some general engineering principles, such as the importance of sulfate balance, are developing. Even so, with concrete technology steadily moving toward these more complex mix designs, it is critical that an engineering/scientific basis be established for understanding and ameliorating compatibility issues.

5.2. Specific research needs

We close this review by enumerating specific research that is needed to make progress in fundamental understanding of, and improved capability to predict, cement hydration kinetics and corresponding development of properties that dictate performance and service life of concrete. These research needs are primarily focused on securing a better understanding of the chemistry and physics of hydration kinetics. However, this kind of scientific progress will not, by itself, translate to real-world impact unless it can be translated into research tools that can be used by cement manufacturers, ready-mixed concrete suppliers, and admixture developers to improve the quality, delivery, and sustainability of their product. Ideally, such tools must enable the materials engineer to predict concrete properties from characteristics of the starting materials that are readily available, such as a "mill sheet" of the composition and the cement particle size distribution.

5.2.1. What are the correct rate-controlling steps and corresponding rate parameters that characterize hydration?

We have tried to conduct this review in terms of basic mechanisms to the extent possible. Nevertheless, it is obvious that a precise, quantitative description of the chemical kinetics is still lacking. As in the introduction of this review, we contend that major progress in understanding hydration kinetics will be best enabled by placing it on the same fundamental ground that gas-phase reactions and certain geochemical processes now enjoy. Perhaps the biggest obstacle preventing this is that *the individual reactions have not been isolated to analyze their mechanisms and rates*. Significant progress has been made in measuring the kinetics of alite dissolution [27,47,56], C–S–H nucleation [27,47] and, to a lesser extent, of C_3A + gypsum hydration [105]. Further knowledge is needed of the actual or apparent equilibrium constants and absolute rate constants (i.e., moles per unit time per unit surface area) of the rate-controlling step in the dissolution of each clinker phase and the nucleation and growth of each hydration product phase. A complete description would also include the temperature dependence of these parameters and, especially for applications such as oil-well cementing, the pressure dependence. This kind of information will likely require the use of novel experimental techniques, such as the use of flow-through reactors for controlling solution chemistry combined with in situ vertical-scanning interferometry [21], and will likely require

integration with *ab initio* modeling [117], molecular modeling methods such as molecular dynamics [118], or kinetic Monte Carlo approaches [10,21,119].

When an SCM like fly ash or blast furnace slag is included, this same kind of information for the SCM will be required. Knowledge of these admixtures is still in its infancy, and to make progress, it will first be necessary to adequately characterize SCMs to improve our understanding of the important chemical factors (aluminate content, heavy metal and other impurities) and structural factors (glassy versus crystalline phases, particle size distribution) that govern the intrinsic reactivity of an SCM. With this characterization, the reaction mechanisms and corresponding rate constants of glassy phases in aqueous solutions – leaching of ions and dissociation of the silicate network – also will be required.

To further complicate the problem, modern concrete formulations invariably contain numerous chemical admixtures (e.g., polycarboxylates and amines) to control workability, setting time, air void content, and shrinkage behavior. More progress likely can be made by systematically examining how hydration rates, and particularly the rates of formation of different hydration products, is influenced by the addition of chemical admixtures. Examples of this approach have already been given in this review [67,68], but much more can be done to characterize the mechanistic influences of admixtures. Interactions of organic molecules with ions in solution (e.g., chelation) and with the inorganic surfaces of cement particles (e.g., adsorption) are not well understood. In some cases it may be permissible to assume that these kinds of interactions occur at rates that are fast compared to other cement hydration reactions, thereby allowing one to assume equilibrium conditions for them. Even so, quantitative modeling will require the knowledge of the equilibrium constants or adsorption isotherms for each important kind of interaction.

Needless to say, obtaining these kinds of fundamental, comprehensive kinetic data is a challenging long-term research proposition that will undoubtedly involve advances in measurement science and technology, including the introduction of new experimental methods and greater integration with fundamental multi-scale computational modeling. But the understanding it will generate might be considered to be the cement equivalent of mapping the human genome. It will allow the understanding and avoidance of compatibility problems that often plague blended cements, as well as the rational control of setting and strength development in the field. Ideally, we envision the development of a shared database containing this kind of information, that could be accessed by researchers worldwide and even updated with more accurate information as it becomes available.

5.2.2. Can chemical kinetics be linked more rigorously to the structure and distribution of hydration products?

Early hydration rates can be modified with temperature or the addition of nucleating agents [67] or other chemical additives [74,90,110,120]. Increased rates of hydration, however, do not necessarily lead to improvements in strength or transport properties at later ages. Controlling both the kinetics *and* the engineering properties of concrete is a great challenge and will require an understanding of how the amount, spatial distribution, and morphology of hydration products are influenced by curing conditions and chemical additives (see Ref. [70] for a thorough visual tour of how morphology of hydration products are influenced by temperature and chemical composition). Progress will undoubtedly be made by combining relevant experimental techniques, such as QENS, SANS, and electron microscopy with advanced multi-scale simulation methods that couple molecular dynamics, Kinetic Monte Carlo, and microstructural models of the rate processes.

Another area of incomplete understanding is the way in which C–S–H growth at the nanoscale, either by aggregation of nanocrystals or frustrated growth of sheets, can result in the wide variety of C–S–H morphologies observed at the microstructural scale [26,49,70,109,121–123], which range from "lamellar" or "fibrillar" to "crumpled foil" to the "Williamson" morphology first reported in Ref. [124], which is a spherulitic type resembling a sheaf of wheat. Recent progress in understanding similar ranges of growth morphologies of solids from polymer melts in terms of fundamental growth mechanisms and the roles of impurities and defects [125], are likely to shed light on larger-scale morphological development of C–S–H.

Acknowledgments

This paper is an outcome of the International Summit on Cement Hydration Kinetics and Modeling. The authors acknowledge financial support from the National Science Foundation (NSF) through Grant Award Nos. OISE-0757284 and CMS-0510854, the Federal Highway Administration (FHWA), Mapei, W. R. Grace, BASF, the Tennessee Technological University (TTU) Center for Manufacturing Research (CMR), the Canadian Research Center on Concrete Infrastructure (CRIB) and the Natural Science and Engineering Research Council of Canada (NSERCC). The authors would also like to acknowledge the organizers of the Summit including Joseph J. Biernacki (TTU), Will Hansen (University of Michigan), and Jacques Marchand (Laval University).

References

[1] H.F.W. Taylor, P. Barret, P.W. Brown, D.D. Double, G. Frohnsdorff, V. Johansen, D. Ménétrier-Sorrentino, I. Odler, L.J. Parrott, J.M. Pommersheim, M. Regourd, J.F. Young, The hydration of tricalcium silicate, Mater. Struct. 17 (1984) 457–468.
[2] E.M. Gartner, J.M. Gaidis, Hydration mechanisms, I, in: J. Skalny (Ed.), Materials Science of Concrete, Vol. 1, American Ceramic Society, Westerville, OH, 1989, pp. 95–125.
[3] J.M. Gaidis, E.M. Gartner, Hydration mechanisms, II, in: J. Skalny, S. Mindess (Eds.), Materials Science of Concrete, Vol. 2, American Ceramic Society, Westerville, OH, 1989, pp. 9–39.
[4] E.M. Gartner, J.F. Young, D.A. Damidot, I. Jawed, Hydration of portland cement, in: J. Bensted, P. Barnes (Eds.), Structure and Performance of Cements, 2nd Edition, Spon Press, New York, 2002, pp. 57–113.
[5] S. Glasstone, K.J. Laidler, H. Eyring, The Theory of Rate Processes, McGraw-Hill, New York, 1941.
[6] D. Kaschiev, G.M. van Rosmalen, Review: nucleation in solutions revisited, Cryst. Res. Technol. 38 (2003) 555–574.
[7] H.H. Teng, P.M. Dove, J.J.D. Yoreo, The kinetics of calcite growth: interpreting chemical affinity-based rate laws through the lens of direct observation, Morphology and Dynamics of Crystal Surfaces in Complex Molecular Systems, Mater. Res. Soc. Symposium Proc, 620, 2000, p. M2.6.
[8] K.J. Davis, P.M. Dove, J.J.D. Yoreo, Resolving the control of magnesium on calcite growth: thermodynamic and kinetic consequences of impurity incorporation for biomineral formation, Morphological and Dynamics of Crystal Surfaces in Complex Molecular Systems, Mater. Res. Soc. Symposium Proc., 620, 2000, p. M.9.5.1.
[9] A.C. Lasaga, Rate laws of chemical reactions, in: A.C. Lasaga, R.J. Kirkpatrick (Eds.), Kinetics of Geochemical Processes, No. 8 in Reviews in Mineralogy, Mineralogical Society of America, 1981, pp. 1–68.
[10] A.C. Lasaga, A. Luttge, Variation of crystal dissolution rate based on a dissolution step wave model, Science 291 (2001) 2400–2404.
[11] R.S. Arvidson, I.E. Ertan, J.E. Amonette, A. Luttge, Variation in calcite dissolution rates: a fundamental problem? Geochim. Cosmochim. Acta 67 (9) (2003) 1623–1634.
[12] P.M. Dove, N. Han, J.J.D. Yoreo, Mechanisms of classical crystal growth theory explain quartz and silicate dissolution behavior, Proc. Nat. Acad. Sci. U.S.A. 102 (43) (2005) 15357–15362.
[13] P.M. Dove, N. Han, Kinetics of mineral dissolution and growth as reciprocal microscopic surface processes across chemical driving force, AIP Conference Proceedings, Vol. 916, 2007, pp. 215–234.
[14] R. Mills, V.M.M. Lobo, Self-Diffusion in Electrolyte Solutions, Elsevier, Amsterdam, 1989.
[15] G.A. Somorjai, Introduction to Surface Chemistry and Catalysis, Wiley-Interscience, New York, 1994.
[16] A.W. Adamson, A.P. Gast, Physical Chemistry of Surfaces, 6th EditionWiley-Interscience, New York, 1997.
[17] W.K. Burton, N. Cabrera, F.C. Frank, The growth of crystals and the equilibrium structure of their surfaces, Phil. Trans. R. Soc. Lond. A 243 (866) (1951) 299–358.
[18] W. Stumm, J.J. Morgan, Aquatic Chemistry, Wiley-Interscience, New York, 1972.
[19] F.M.M. Morel, Principles of Aquatic Chemistry, Wiley-Interscience, New York, 1983.

[20] R.S. Arvidson, C. Fischer, A. Luttge, Resolution of crystal dissolution and growth processes at multiple scales, Geochim. Cosmochim. Acta 72 (12) (2009) A34.
[21] J. Cama, L. Zhang, G. De Guidici, J.M. Soler, R.S. Arvidson, A. Luttge, Dissolution of fluorite (111) cleavage surface in acid pH: VSI, AFM, and Monte Carlo simulations, Geochim. Cosmochim. Acta 73 (2009) A187.
[22] C.C. Battaile, D.J. Srolovitz, J.E. Butler, A kinetic Monte Carlo method for the atomic-scale simulation of chemical vapor deposition: application to diamond, J. Appl. Phys. 82 (12) (1997) 6293–6300.
[23] V.B. Shenoy, R. Miller, E.B. Tadmor, R. Phillips, M. Ortiz, An adaptive finite element approach to atomic-scale mechanics—the quasicontinuum method, J. Mech. Phys. Solids 47 (3) (1999) 611–642.
[24] L. Gránásy, T. Pusztai, T. Borzsonyi, J.A. Warren, J.F. Douglas, A general mechanism of polycrystalline growth, Nat. Mater. 3 (9) (2004) 645–650.
[25] K. Muralidharan, J.H. Simmons, P.A. Deymier, K. Runge, Molecular dynamics studies of brittle fracture in vitreous silica: review and recent progress, J. Non-Cryst. Solids 351 (18) (2005) 1532–1542.
[26] M.M. Costoya, Effect of particle size on the hydration kinetics and microstructural development of tricalcium silicate, PhD dissertation, École Polytechnique Fédérale de Lausanne, Lausanne, Switzerland, 2008.
[27] S. Garrault, A. Nonat, Hydrated layer formation on tricalcium and dicalcium silicate surfaces: experimental study and numerical simulations, Langmuir 17 (2001) 8131–8138.
[28] V. Kocaba, Development and evaluation of methods to follow microstructural development of cementitious systems including slags, PhD dissertation, École Polytechnique Fédérale de Lausanne, Lausanne, Switzerland, 2009.
[29] J.J. Thomas, H.M. Jennings, A.J. Allen, The surface area of cement paste as measured by neutron scattering — evidence for two C–S–H morphologies, Cem. Concr. Res. 28 (1998) 897–905.
[30] J.J. Thomas, A.J. Allen, H.M. Jennings, Hydration kinetics and microstructure development of normal and $CaCl_2$-accelerated tricalcium silicate (C_3S) pastes, J. Phys. Chem. C 113 (2009) 19836–19844.
[31] S.A. FitzGerald, D.A. Neumann, J.J. Rush, D.P. Bentz, R.A. Livingston, In situ quasi-elastic neutron scattering study of the hydration of tricalcium silicate, Chem. Mater. 10 (1998) 397.
[32] J.J. Thomas, S.A. FitzGerald, D.A. Neumann, R.A. Livingston, State of water in hydrating tricalcium silicate and portland cement pastes as measured by quasi-elastic neutron scattering, J. Am. Ceram. Soc. 84 (8) (2001) 1811–1816.
[33] D.L. Parkhurst, User's guide to PHREEQC—a computer program for speciation reaction-path, advective-transport, and geochemical calculations, Water-Resources Investigations Report 95-4227, U.S. Geological Survey, 1995.
[34] W. Hummel, U. Berner, E. Curti, F.J. Pearson, T. Thoenen, Nagra/PSI Chemical Thermodynamic Data Base 01/01, Universal Publishers, Parkland, Florida, 2002.
[35] P. Barret, D. Ménétrier, Filter dissolution of C_3S as a function of the lime concentration in a limited amount of lime water, Cem. Concr. Res. 10 (1980) 521–534.
[36] P. Barret, D. Ménétrier, D. Bertrandie, Mechanism of C_3S dissolution and problem of the congruency in the very initial period and later on, Cem. Concr. Res. 13 (1983) 728–738.
[37] J.B. Ings, P.W. Brown, G. Frohnsdorff, Early hydration of large single crystals of tricalcium silicate, Cem. Concr. Res. 13 (1983) 843–848.
[38] D. Damidot, A. Nonat, C_3S hydration in dilute and stirred suspensions: (I) study of the two kinetic steps, Adv. Cem. Res. 6 (21) (1994) 27–35.
[39] D. Damidot, F. Bellmann, B. Möser, T. Sovoidnich, Calculation of the dissolution rate of tricalcium silicate in several electrolyte compositions, Cement Wapno Beton 12/74 (2) (2007) 57–67.
[40] H.N. Stein, Thermodynamic considerations on the hydration mechanisms of Ca_3SiO_5 and $Ca_3Al_2O_6$, Cem. Concr. Res. 2 (2) (1972) 167–177.
[41] E.M. Gartner, H.M. Jennings, Thermodynamics of calcium silicate hydrates and their solutions, J. Am. Ceram. Soc. 80 (10) (1987) 743–749.
[42] H.N. Stein, J.M. Stevels, Influence of silica on the hydration of 3CaO, SiO2, J. Appl. Chem. 14 (1964) 338–346.
[43] H.M. Jennings, P.L. Pratt, An experimental argument for the existence of a protective membrane surrounding portland cement during the induction period, Cem. Concr. Res. 9 (1979) 501–506.
[44] H.M. Jennings, Aqueous solubility relationships for two types of calcium silicate hydrate, J. Am. Ceram. Soc. 69 (8) (1986) 614–618.
[45] J.W. Bullard, A determination of hydration mechanisms for tricalcium silicate using a kinetic cellular automaton model, J. Am. Ceram. Soc. 91 (7) (2008) 2088–2097.
[46] R. Kondo, S. Ueda, Kinetics and mechanisms of the hydration of cements, Proceedings of the Fifth International Symposium on the Chemistry of Cement, Volume 2, 1968, pp. 203–212.
[47] S. Garrault-Gauffinet, A. Nonat, Experimental investigation of calcium silicate hydrate (C–S–H) nucleation, J. Cryst. Growth 200 (1999) 565–574.
[48] R.A. Livingston, J.S. Schweitzer, C. Rolfs, H.W. Becker, S. Kubsky, Characterization of the induction period in tricalcium silicate hydration by nuclear resonance reaction analysis, J. Mater. Res. 16 (3) (2001) 687–693.
[49] J.W. Schweitzer, R.A. Livingston, C. Rolfs, H.W. Becker, S. Kubsky, T. Spillane, M. Castellote, P.G. de Viedma, In situ measurements of the cement hydration profile during the induction period, Proceedings of the Twelfth International Congress on the Chemistry of Cement, National Research Council of Canada, Montreal, Canada, 2007.
[50] H.F.W. Taylor, Cement Chemistry, 2nd Edition. Thomas Telford, London, 1997.
[51] F. Bellmann, D. Damidot, B. Möser, J. Skibsted, Improved evidence for the existence of an intermediate phase during hydration of tricalcium silicate, Cem. Concr. Res. 40 (2010) 875–884.
[52] N.J. Clayden, C.M. Dobson, C.J. Hayes, S.A. Rodger, Hydration of tricalcium silicate followed by solid-state ^{29}Si NMR spectroscopy, J. Chem. Soc. Chem. Commun. 21 (1984) 1396–1397.
[53] S.A. Rodger, G.W. Groves, N.J. Clayden, C.M. Dobson, Hydration of tricalcium silicate followed by ^{29}Si NMR with cross polarization, J. Am. Ceram. Soc. 71 (1988) 91–96.
[54] X.D. Cong, R.J. Kirkpatrick, ^{17}O and ^{29}Si MAS NMR study of β-C_2S hydration and the structure of calcium silicate hydrates, Cem. Concr. Res. 23 (1993) 1065–1077.
[55] S. Garrault, E. Finot, E. Lesniewska, A. Nonat, Study of C–S–H growth on C3S surface during its early hydration, Mater. Struct. 38 (2005) 435–442.
[56] P. Juilland, E. Gallucci, R. Flatt, K. Scrivener, Dissolution theory applied to the induction period in alite hydration, Cem. Concr. Res. 40 (2010) 831–844.
[57] D. Damidot, A. Nonat, P. Barret, Kinetics of tricalcium silicate hydration in diluted suspensions by microcalorimetric measurements, J. Am. Ceram. Soc. 73 (11) (1990) 3319–3322.
[58] A. Nonat, Modelling hydration and setting of cement, Ceramics 92 (2005) 247–257.
[59] T. Sakurai, T. Sato, A. Yoshinaga, The effect of minor components on the early hydraulic activity of the major phases of portland cement clinker, Proceedings of the Fifth International Symposium on the Chemistry of Cement,Vol. 1 Tokyo, Japan, 1968, pp. 300–321.
[60] D. Ménétrier, I. Jawed, T.S. Sun, J. Skalny, ESCA and SEM studies on early C_3S hydration, Cem. Concr. Res. 9 (1979) 473–482.
[61] J.M. Makar, G.W. Chan, End of induction period in ordinary portland cement as examined by high-resolution scanning electron microscopy, J. Am. Ceram. Soc. 91 (2008) 1292–1299.
[62] P. Fierens, J.P. Verhaegen, Induction period of hydration of tricalcium silicate, Cem. Concr. Res. 2 (1976) 287–292.
[63] I. Odler, J. Schüppstuhl, Early hydration of tricalcium silicate 3. Control of the induction period, Cem. Concr. Res. 11 (1981) 765–774.
[64] J.N. Maycock, J.P. Skalny, R.S. Kalyoncu, Solid-state defects and clinker mineral hydration, Am. Ceram. Soc. Bull. 53 (1974) 326.
[65] J.J. Thomas, A new approach to modeling the nucleation and growth kinetics of tricalcium silicate hydration, J. Am. Ceram. Soc. 90 (10) (2007) 3282–3288.
[66] S. Bishnoi, K.L. Scrivener, μic: A new platform for modelling the hydration of cements, Cem. Concr. Res. 39 (4) (2009) 266–274.
[67] J.J. Thomas, H.M. Jennings, J.J. Chen, Influence of nucleation seeding on the hydration mechanisms of tricalcium silicate and cement, J. Phys. Chem. C 113 (11) (2009) 4327–4334.
[68] J.W. Bullard, R.J. Flatt, New insights into the effect of calcium hydroxide precipitation on the kinetics of tricalcium silicate hydration, J. Am. Ceram. Soc. 93 (2010) 1894–1903.
[69] S. Gauffinet, E. Finot, R. Lesniewska, A. Nonat, Direct observation of the growth of calcium silicate hydrate on alite and silica surfaces by atomic force microscopy, C. R. Acad. Sci. Paris Earth Planet. Sci. 327 (4) (1998) 231–236.
[70] I.G. Richardson, Tobermorite/jennite- and tobermorite/calcium hydroxide-based models for the structure of C–S–H: applicability to hardened pastes of tricalcium silicate, β-dicalcium silicate, portland cement, and blends of portland cement with blast-furnace slag, metakaolin, or silica fume, Cem. Concr. Res. 34 (2004) 1733–1777.
[71] M. Zajac, Étude des relations entre vitesse d'hydratation, texturation des hydrates et résistance méchanique finale des pâtes et micro-mortiers de ciment portland. PhD dissertation, Universite de Bourgogne, Dijon, France, 2007.
[72] J.J. Thomas, J.J. Biernacki, J.W. Bullard, S. Bishnoi, J.S. Dolado, G.W. Scherer, A. Luttge, Modeling and simulation of cement hydration kinetics and microstructure development, Cem. Concr. Res. 41 (2011) 1257–1278.
[73] A.J. Allen, J.C. McLaughlin, D.A. Neumann, R.A. Livingston, In situ quasi-elastic scattering characterization of particle size effects on the hydration of tricalcium silicate, J. Mater. Res. 19 (11) (2004) 3242–3254.
[74] V.K. Peterson, M.C.G. Juenger, Hydration of tricalcium silicate: effects of $CaCl_2$ and sucrose on reaction kinetics and product formation, Chem. Mater. 18 (2006) 5798–5804.
[75] G.W. Scherer, J. Zhang, and J.J. Thomas, Nucleation and Growth Models for Hydration of Cement, in preparation.
[76] J. Zhang, E.A. Weissinger, S. Peethamparan, G.W. Scherer, Early hydration and setting of oil well cement, Cem. Concr. Res. 40 (2010) 1023–1033.
[77] Z.Q. Wu, J.F. Young, The hydration of tricalcium silicate in the presence of colloidal silica, J. Mater. Sci. 19 (1984) 3477–3486.
[78] A.J. Allen, R.C. Oberthur, D. Pearson, P. Schofield, C.R. Wilding, Development of the fine porosity and gel structure of hydrating cement systems, Philos. Mag. B 56 (1987) 263–268.
[79] H.M. Jennings, A model for the microstructure of calcium silicate hydrate in cement paste, Cem. Concr. Res. 30 (2000) 101–116.
[80] A.J. Allen, J.J. Thomas, H.M. Jennings, Composition and density of nanoscale calcium–silicate–hydrate in cement, Nat. Mater. 6 (2007) 311–316.
[81] H.M. Jennings, J.J. Thomas, J.S. Gevrenov, G. Constantinides, F.-J. Ulm, A multi-technique investigation of the nanoporosity of cement paste, Cem. Concr. Res. 37 (2007) 329–336.
[82] H.M. Jennings, J.W. Bullard, J.J. Thomas, J.E. Andrade, J.J. Chen, G.W. Scherer, Characterization and modeling of pores and surfaces in cement paste: correlations to processing and properties, J. Adv. Concr. Technol. 6 (1) (2008) 1–25.
[83] E.M. Gartner, A proposed mechanism for the growth of C–S–H during the hydration of tricalcium silicate, Cem. Concr. Res. 27 (5) (1997) 665–672.
[84] G. Constantinides, F.-J. Ulm, The effect of two types of C–S–H on the elasticity of cement-based materials: results from nanoindentation and micromechanical modeling, Cem. Concr. Res. 34 (2004) 67–80.

[85] G. Constantinides, F.-J. Ulm, The nanogranular nature of C–S–H, J. Mech. Phys. Solids 55 (2007) 64–90.
[86] S. Bishnoi, K.L. Scrivener, Studying nucleation and growth kinetics of alite hydration using μic, Cem. Concr. Res. 39 (2009) 849–860.
[87] J.F. Young, H.S. Tong, R.L. Berger, Composition of solutions in contact with hydrating tricalcium silicate pastes, J. Am. Ceram. Soc. 60 (1977) 193–198.
[88] I. Jawed, J. Skalny, Surface phenomena during tricalcium silicate hydration, J. Colloid Interface Sci. 85 (1) (1982) 235–243.
[89] I. Odler, H. Dörr, Early hydration of tricalcium silicate II. The induction period, Cem. Concr. Res. 9 (1979) 277–284.
[90] P.W. Brown, C.L. Harner, E.J. Prosen, The effect of inorganic salts on tricalcium silicate hydration, Cem. Concr. Res. 16 (1985) 17–22.
[91] J.G.M. de Jong, H.N. Stein, J.M. Stevels, Hydration of tricalcium silicate, J. Appl. Chem. 17 (1967) 246–250.
[92] K.L. Scrivener, The development of microstructure during hydration of portland cement. Ph.D. Dissertation, University of London, 1984.
[93] T. Knudsen, Kinetics of the reaction of β-C_2S and C_3S with CO_2 and water vapor, J. Am. Ceram. Soc. 63 (1980) 114–115.
[94] V.K. Peterson, D.A. Neumann, R.A. Livingston, Hydration of tricalcium and dicalcium silicate mixtures studied using quasielastic neutron scattering, J. Phys. Chem. B 109 (2005) 14449–14453.
[95] A.J. Allen, R.C. Oberthur, D. Pearson, P. Schofield, C.R. Wilding, Development of the fine porosity and gel structure of hydrating cement systems, Philos. Mag. B 56 (1987) 263–288.
[96] A.J. Allen, Time-resolved phenomena in cements, clays, and porous rocks, J. Appl. Cryst. 24 (1991) 624–634.
[97] K. Mori, et al., Observation of microstructure of hydrated Ca_3SiO_5, Phys. B Condensed Matter 385 (2006) 517–519.
[98] D.W. Hadley, W.L. Dolch, S. Diamond, On the occurrence of hollow-shell hydration grains in hydrated cement paste, Cem. Concr. Res. 30 (2000) 1–6.
[99] K.O. Kjellsen, B. Lagerblad, Microstructure of tricalcium silicate and portland cement systems at middle periods of hydration-development of Hadley grains, Cem. Concr. Res. 37 (2007) 13–20.
[100] E. Gallucci, P. Mathur, K.L. Scrivener, Microstructural development of early age hydration shells around cement grains, Cem. Concr. Res. 40 (2010) 4–13.
[101] R.A. Livingston, N. Nemes, D.A. Neumann, The transition point in the hydration kinetics of tricalcium silicate determined by quasi-elastic neutron scattering, unpublished.
[102] W.A. Corstanje, H.N. Stein, J.M. Stevels, Hydration reactions in pastes $C_3S + C_3A + CaSO_4.2aq + H_2O$ at 25 °C, Cem. Concr. Res. 3 (1973) 791–806.
[103] W.A. Corstanje, H.N. Stein, J.M. Stevels, Hydration reactions in pastes $C_3S + C_3A + CaSO_4.2aq + H_2O$ at 25 °C III, Cem. Concr. Res. 4 (1974) 417–431.
[104] E. Breval, C_3A hydration, Cem. Concr. Res. 6 (1976) 129–138.
[105] H. Minard, S. Garrault, L. Regnaud, A. Nonat, Mechanisms and parameters controlling the tricalcium aluminate reactivity in the presence of gypsum, Cem. Concr. Res. 37 (2007) 1418–1426.
[106] N. Tenoutasse, The hydration mechanism of C_3A and C_3S in the presence of calcium chloride and calcium sulphate, Proceedings of the Fifth International Symposium on the Chemistry of Cement, Volume II, The Cement Association of Japan, Tokyo, Japan, 1968, pp. 372–378.
[107] K.L. Scrivener, P.L. Pratt, Microstructural studies of the hydration of C_3A and C_4AF independently and in cement paste, in: F.P. Glasser (Ed.), Brit. Ceram. Proc. 35, Stoke-on-Trent, British Ceramic Society, 1984, pp. 207–219.
[108] W. Lerch, The influence of gypsum on the hydration reactions of portland cement, Proc. ASTM 46 (1946) 1252–1292.
[109] D.P. Bentz, Influence of silica fume on diffusivity in cement-based materials. I. Experimental and computer modeling studies on cement pastes, Cem. Concr. Res. 30 (2000) 953–962.
[110] D.D. Double, New developments in understanding the chemistry of cement hydration, Phil. Trans. R. Soc. Lond. A 310 (1983) 53–66.
[111] H.M. Jennings, B.J. Dalgleish, P.L. Pratt, Morphological development of hydrating tricalcium silicate as examined by electron microscopy techniques, J. Am. Ceram. Soc. 64 (10) (1981) 567–572.
[112] P.L. Pratt, H.M. Jennings, The microchemistry and microstructure of portland cement, Ann. Rev. Mater. Sci. 11 (1981) 123–149.
[113] R.D. Coatman, N.L. Thomas, D.D. Double, Studies of the growth of silicate gardens and related phenomena, J. Mater. Sci. 15 (1980) 2017-2026.
[114] E.E. Lachowski, S. Diamond, Investigation of the composition and morphology of individual particles of portland cement paste. 1. C–S–H gel and calcium hydroxide particles, Cem. Concr. Res. 13 (1983) 177–185.
[115] S. Diamond, E.E. Lachowski, Investigation of the composition and morphology of individual particles of portland cement paste. 2. Calcium sulfoaluminates, Cem. Concr. Res. 13 (1983) 335–340.
[116] B. Lothenbach, et al., Supplementary cementitious materials, Cem. Concr. Res. 41 (2011) 1244–1256.
[117] A. Lasaga, G.V. Gibbs, Ab initio quantum mechanical calculations of water–rock interactions: adsorption and hydrolysis reactions, Am. J. Sci. 290 (1990) 263–295.
[118] S.C. Parker, N.H. de Leeuw, E. Bourova, D.J. Cooke, Application of lattice dynamics and molecular dynamics techniques to minerals and their surfaces, in: R.T. Cygan, J.D. Kubicki (Eds.), Molecular Modeling Theory: Applications in the Geosciences, Reviews in Mineralogy and Geochemistry, 42, Mineralogical Society of America, Washington, D.C, 2001, pp. 63–82.
[119] A. Luttge, Crystal dissolution kinetics studied by vertical scanning interferometry and Monte Carlo simulations, in: X.-Y. Liu, J.J. De Yoreo (Eds.), Interfacial Structures versus Dynamics, Series on Nanoscience and Technologies, Vol. I, Kluwer Academic Publisher, New York, 2004, pp. 209–247.
[120] P. Bénard, S. Garrault, A. Nonat, C. Cau-dit-Coumes, Influence of orthophosphate ions on the dissolution of tricalcium silicate, Cem. Concr. Res. 38 (2008) 1137–1141.
[121] M.C.G. Juenger, V.H.R. Lamour, P.J.M. Monteiro, E.M. Gartner, G.P. Denbeaux, Direct observation of cement hydration by soft X-ray transmission microscopy, J. Mater. Sci. Lett. 22 (19) (2003) 1335–1337.
[122] M.C.G. Juenger, P.J.M. Monteiro, E.M. Gartner, G.P. Denbeaux, A soft X-ray microscope investigation into the effects of calcium chloride on tricalcium silicate hydration, Cem. Concr. Res. 35 (1) (2005) 19–25.
[123] D.A. Silva, P.J.M. Monteiro, Hydration evolution of C_3S–EVA composites analyzed by soft X-ray microscopy, Cem. Concr. Res. 35 (2005) 351–357.
[124] R.B. Williamson, Constitutional supersaturation in portland cement solidified by hydration, J. Cryst. Growth 3 (1968) 787–794.
[125] L. Gránásy, T. Pusztai, G. Tegze, J.A. Warren, J.F. Douglas, Growth and form of spherulites, Phys. Rev. E 72 (2006) 011605.
[126] P. Barret, D. Ménétrier, D. Bertrandie, M. Regourd, Comparative study of C–S–H formation from supersaturated solutions and C_3S solution mixtures, 7th International Congress on the Chemistry of Cement, Paris, France, 1980.